

content samples for Li along Tamogh River suggests that those pegmatites may contain mica relatively high in Li contents.

The fact that no anomalous sample possibly reflecting the mineralization has not been found in the area is consistent with the field observation that abundant pegmatites are all barren for any useful metal mineralization.

## 2-4 Detailed Survey Area

The area occupies an area of 10 km<sup>2</sup> for geological survey and includes an area of 3 km<sup>2</sup> for geochemical survey (Fig. 2). It covers the Telot serpentinite body in which the chromium, nickel and gold deposits occur.

The main object of the survey was to study the mineralization of chromium, nickel and gold and determine the scale and form of the deposits.

### 2-4-1 Geology

The geology of the area comprises metamorphic and intrusive rocks. The metamorphic rocks consist of the M-3 formation and the M-4 formation of the Mozambique belt metamorphic rocks (corresponding to the Basement III formation and the Basement IV formation as classified in the survey report of the Phase I). The main rock facies are hornblende schist, hornblende gneiss, green schist (actinolite schist and chlorite schist), quartzitic rock, and biotite gneiss. The intrusive rocks include serpentinites and talc schists.

The geological map and sections are shown in Fig. 2-24.

#### (1) Mozambique Belt Metamorphic Rocks

##### M-3 Formation

The main rock facies are fine-grained biotite gneiss (P-mg<sup>b</sup> (III)) and quartzite (P-mq(IV)), interbedded with thin layers of chlorite schist (P-ms<sup>c</sup> (III)), hornblende gneiss (P-mg<sup>h</sup> (III)) and graphite schist (P-ms<sup>I</sup> (III)). Biotite gneiss contains locally muscovite, hornblende and garnet (less than 10 mm in diameter) and porphyroblasts of potash-feldspar (less than 5 mm in diameter).

The thickness of the M-3 formation is estimated to be 300 m (+) in the area.

##### M-4 Formation

The M-4 formation occupies the widest part in the area. From the point of view of rock facies, the green schist (P-ms<sup>c</sup> (IV)), including actinolite schist and chlorite schist, are dominant, followed by hornblende schist, hornblende gneiss (P-ms<sup>h</sup> (IV)), quartzitic rocks (P-mq (IV)) and hornblende-garnet porphyroblast with two mica-quartz schist (P-ms<sup>ghmq</sup> (IV)). Biotite gneiss (P-mg<sup>b</sup> (IV)) has been observed only in form of thin layers.





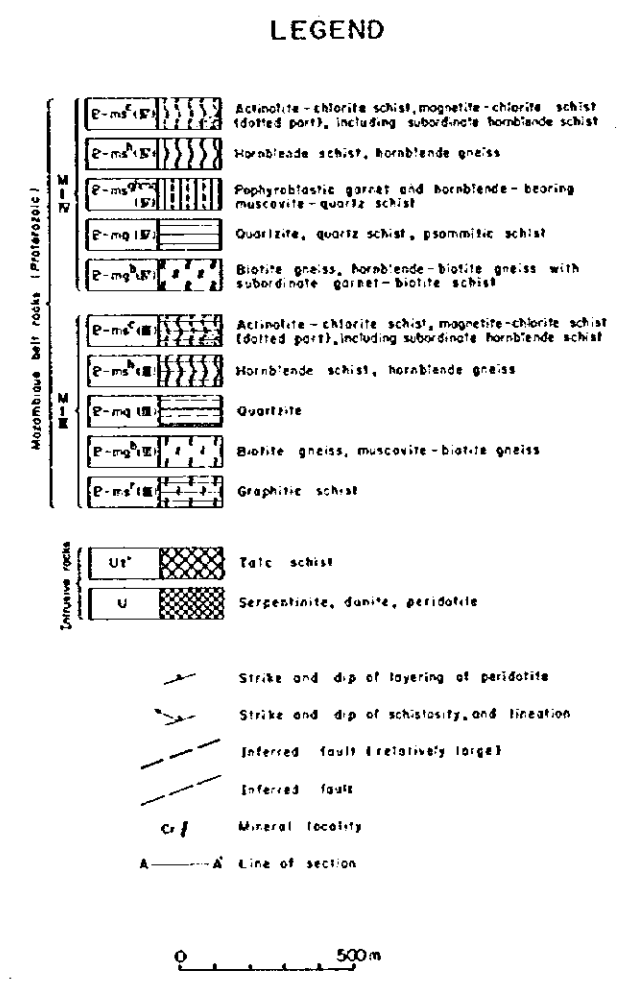
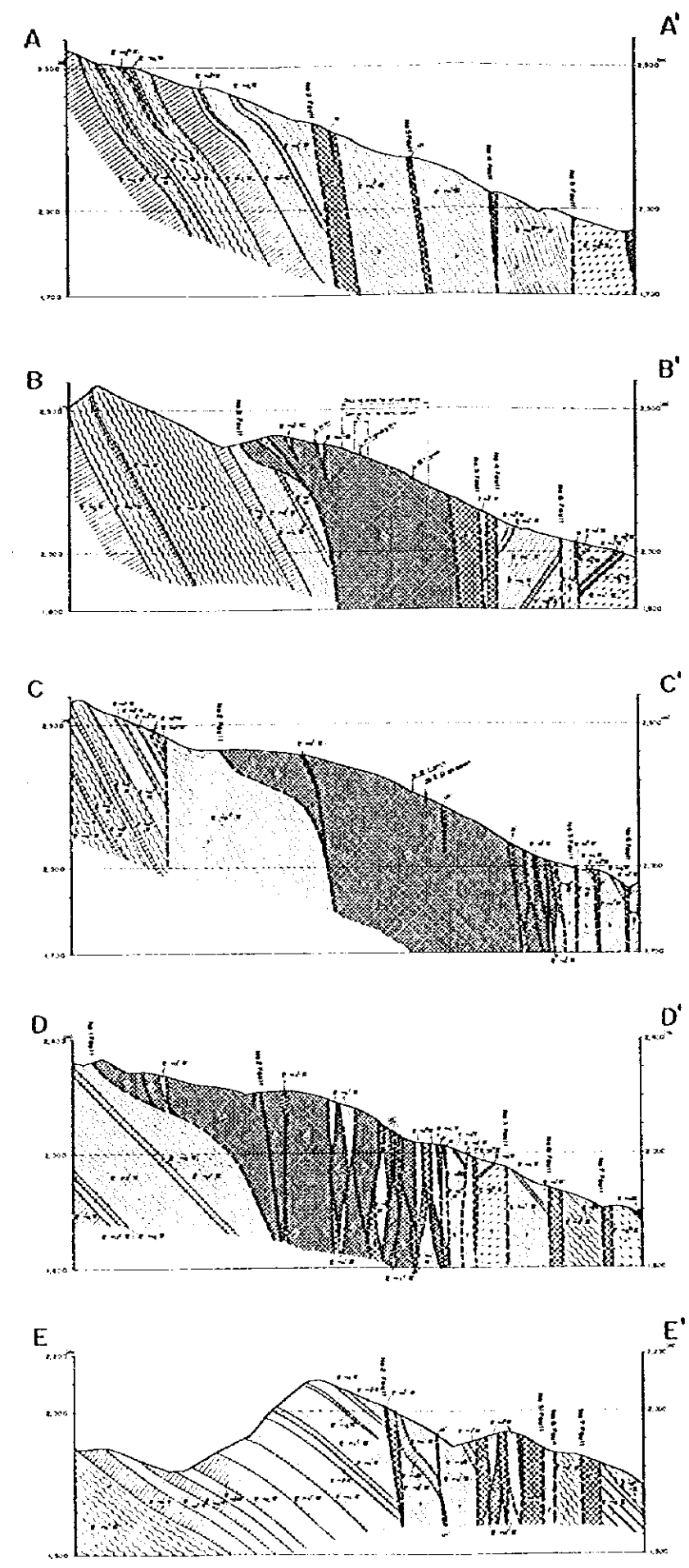
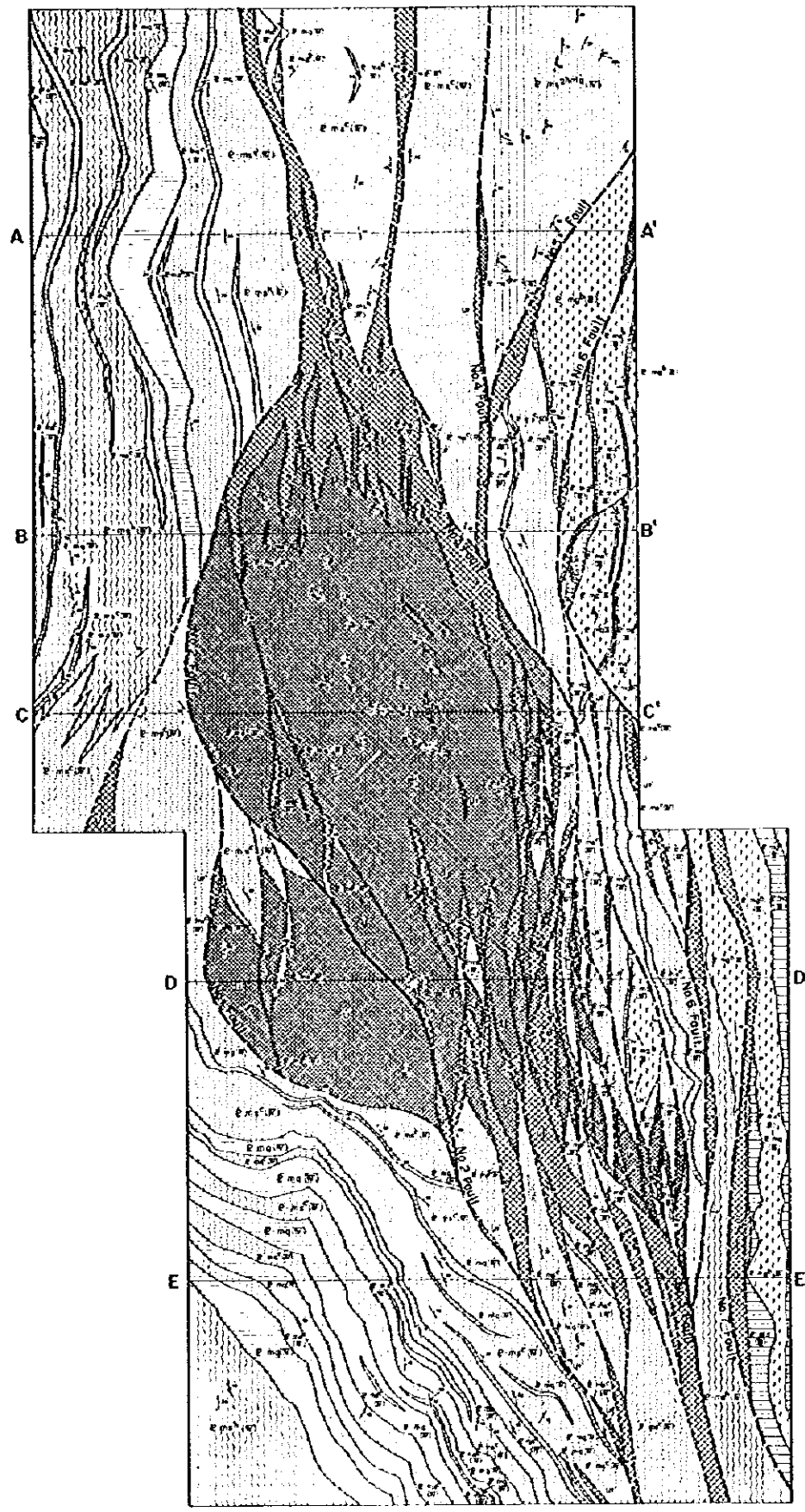


Fig. 2-24 Geological Map and Sections, Detailed Survey Area



The green schists which are considered to have been formed from the hornblende gneisses by retrogressive metamorphism, are fine-grained rocks with a marked schistosity and consist of chlorite-actinolite schist and chlorite schist.

## (2) Intrusive Rocks

### Serpentinites

Serpentinites (U) occur as lenticular intrusive bodies in metamorphic rocks and talc schist. The form and distribution of serpentinite bodies were investigated very precisely during the survey. They are classified into a large serpentinite body (Telot serpentinite body) and about thirty other small bodies. The Telot serpentinite body extends for about 2.5 km northwards with a width of about 1 km showing an elliptical form, and area of exposure is about 2 km<sup>2</sup>.

In northern and southern limits, the exposure of the body terminates abruptly showing an intricate form intercalating a large amount of green schist and talc schist. It is likely that the abrupt termination resulted from the development of faults. The western side of the body is bordered by Telot No. 1 and No. 2 faults, and shows a relatively distinct boundary. On the eastern side, occurrence of many small faults led to intricate distribution of lenticular small bodies of serpentinite, talc schist and green schist making the boundary of Telot serpentinite body indistinct.

Many of the small bodies are several tens of meters wide and 200 to 300 meters long. About twenty bodies are distributed in a relatively concentrated form on the southeast of the Telot serpentinite body, others are scattered along the faults.

The degree of serpentinization is varied from the fresh rock in which olivine occupies 80 to 90 percent to the rock that is wholly serpentine. The part containing chromite has been highly serpentinized, having been completely altered to antigorite serpentinite. Antigorite, talc and calcite are observed as secondary minerals associated with serpentinization. Dunite, wehrlite and lehrzomite have been identified as the original rocks of serpentinite under the microscope.

From chemical composition by whole rock analysis the high MgO/total FeO ratios over 7.5 indicates that the Telot serpentinite body is relatively poor in Fe content as chemical characteristics.  $\text{MgO} \times 100 / (\text{MgO} + \text{total FeO})$  ratios are 88 to 89% and are plotted in the field of the Alpine type ultramafic rocks. In the MgO-CaO-Al<sub>2</sub>O<sub>3</sub> diagram, both are shown near the MgO apex, included in the field of metamorphic peridotite by Coleman (1977).

### Talc Schists

Talc schists (Ut') are distributed as lenticular to bedded-form intrusive bodies, or associated with serpentinites. Most of the talc schists in the area are considered to have intruded in an inconsistent relationship to the metamorphic rocks. Although the width of the exposure is less than

100 meters, it shows a wide distribution at the point where it is tangled with serpentinite in the northern part of the Telot serpentinite body. The rocks are well spread along the direction of elongation reaching up to 2 kilometers or more in maximum.

Talc schists are white to pale grey and weakly schistose. Vesicles coated by iron oxide are often observed. In parts of high crystallinity, pale green foliated talc crystals several centimeters in diameter are observable. Talc schists containing anthophyllite are reported in the existing literature (McCall, 1964).

Since talc is a common mineral derived by alteration of nonaluminous magnesium silicate in basic or ultrabasic rocks, or by metamorphism of dolomitic rocks, the original rock of talc schist is considered to be ultrabasic rocks closely associated with the rock.

### (3) Geological Structure

The Detailed Survey Area contains a tectonic zone extending in the direction of N-S or NNW-SSE, and the activity of the tectonic zone seems to have resulted in the formation of many faults, intrusion of serpentinite and talc schist, and the formation of green schist subjected to retrogressive metamorphism.

The most prominent structure is the Endogh-Telot overturned synclinal fold which restricts the distribution of rocks in the area. It is difficult to show the location of the axial part on the geological map because the axial part has overlapped the tectonic zone. It is most likely that the synclinal axis is located between the Telot No. 2 fault and the No. 3 fault.

There are many faults in the Telot serpentinite body. Among these faults, seven faults named as No. 1 to No. 7 have good continuity and great amount of displacement. They are shown on the geological map.

### 2-4-2 Ore Deposits

The chromium and nickel deposits at Telot were first discovered in 1956. Since then exploration has been carried out by organizations including New Consolidated Gold Field Ltd. of South Africa, Department of Mines and Geology of Kenya and Japanese consortium constituted by Nippon Kokan KK., Kokan Kogyo KK. and C. Itoh and Co. Ltd. The outline and conclusion of these exploration works are shown in Table 2-16.

On the other hand, although it is said that the gold deposit has been mined since before independence of Kenya in 1963, there is no description for the gold deposit in those exploration reports mentioned above, and it is thought that the panning of gold has become active in recent years.

Table 2-16 Summary of Exploration Work for Telot Cr, Ni, Au Deposits

Investigator Item	New Consolidated Gold Fields Limited	Department of Mines and Geology	Nippon Kokan K.K. Kokan Mining Co., Ltd. C. Itch & Co., Ltd.	MAAJ & JICA (Phase I)
Period of Investigation	April 1957 ~ March 1958	Dec. 1967 ~ Sept. 1968	April 1976 ~ May 1977	Oct. 1983 ~ March 1984
Road Construction Road Repairment, Improvement	Landrover Truck 7 mile (11.26 km)	7 mile (11.26 km)	14 km	
Topographic Survey	Grid-line control	Picketting 3,000ft x 6,000ft 200-foot grid		
Geological Survey Geophysical Survey	120 mi <sup>2</sup> (310 km <sup>2</sup> )	About 3 km <sup>2</sup> (?)  Grand Magnetic Survey 32,000 line feet, 100-foot interval	20 km <sup>2</sup>	120 km <sup>2</sup> (Semi-Detailed Survey)
Trench Excavation Pit Work Tunnel	5,800 Cubic Yards (4,434 m <sup>3</sup> )	500 feet Av. width 3~4 ft Av. depth 5~6 ft	1,380 m 67 pits 122.80 m	Clearing of old Trenches
Diamond Drill Hole		11 winkle DDHs (Total 289 ft)	11 DDHs (Total 412.07 m)	
Analysis	319 soil samples for Ni, Co Some Cr-Ore	58 samples for Cr, Ni	46 samples for Cr, Fe, Ni, Au, Ag, Pt	206 soil samples for Cr, Ni, Co, V, Pt, 61 soil samples for Au 6 samples for Au, Ag 20 samples for Cu, Pt, V, Fe, Al 21 samples for Co, Ni, Cu
Main Targets	Chrome, Nickel	Chrome, Nickel	Chrome	Chrome, Nickel, Gold
Ore reserves of chromite deposit	Total tonnage proved 3,000 tons	Proven reserves 23,000 Long tons Probable reserves 6,500 Long tons Possible reserves 40,000 Long tons Average grade 49.17% Cr <sub>2</sub> O <sub>3</sub> Average Cr/Fe ratio 3.12/1	Main ore body 3,600 tons Total of float ore 3,800 tons Grand total of proved reserves 7,400 tons Probable ore reserves 1,000 tons Proved + Probable 8,400 tons 48% Cr <sub>2</sub> O <sub>3</sub>	The reserves of a single body might be in the order of few to several thousand tons.
Ore reserves of nickel deposit	Total tonnage 8,000,000 tons Averaging a little over 1.0% Ni.	Probable indicated reserves 5,333,000 Long tons Grade slightly more than 1%  Possible indicated reserves 14,425,000 Long tons Average grade 0.7% Ni.	No calculation	No calculation
Conclusion	The prospect does not appear to be economic at ruling prices.	Further development work in order to increase proven chromite reserves and to up-grade present possible indicated reserves to category of proven reserves of nickel is justified.	The development of telot chromite depo- sit will not be profitable. Exploitation of nickel ore will not be economical.	Further detailed geochemical and geological exploration works for nickel and gold mineralization are recommended.



## (1) Chromite

Two major massive chromite lenses, No. 1 and 2 Veins, have so far been located by the previous explorations.

The two occur apparently en echelon within a distance of about 130 m (NNW-SSE): Each strikes  $N15^{\circ}-30^{\circ}E$  and dips steeply to the west (No. 2) or vertical (?). The dimension of the No. 2 vein in the trench is 21 m long with an average width of ca. 1.7 m measured on a 1 m-interval (maximum 4 m), having a ca.  $35.1 \text{ m}^2$  area on plan. This gives reserves of 158 t/vertical m, assuming 4.5 for specific gravity. The dimension of the No. 1 is uncertain, as the surface is now covered by debris, soil etc. However, it is likely to be of the same order to No. 2. Therefore, the reserves of a single body might be in the order of a few to several thousand tonnes, if the depth is assumed 10 to 30 m. As a whole, it may be estimated that up to several bodies might occur within the prospect.

The average grades from five samples which were taken on a 5 m-interval from No. 2 vein are as follows.

33.27% Cr, 12.71% Fe, 2.36% Al, Cr/Fe = 2.62

length = 21 m, average width = 1.41 m (1.71 m when measured on a 1 m interval)

The average grades for four stock piles which are weighted by each volume are as follows.

36.67% Cr, 14.8% Fe, 2.4% Al, Cr/Fe = 2.67

The detail of occurrence and assay results are shown in Fig. 2-25.

The Japanese consortium explored the chromite deposits with diamond drilling works of eleven holes totalling 412 meters. The results showed that the ore bodies are podiform deposits pinching out suddenly downwards, and the calculation of ore reserve is 8,400 tons ( $\text{Cr}_2\text{O}_3$ ) of both proved and probable ore reserves altogether.

The deposit is high in chromium grade and suitable for open pit mining, but scanty in ore reserves, so that the deposit would be acceptable for mining on a small scale for a short time when domestic demand for chromite arises in Kenya, depending on the market conditions.

## (2) Ni

A geological sketch of the trench excavated at the nickel rich zone of the deposits is shown in Fig. 2-26, 2-27 and the typical columnar section of the Telot nickel deposits are shown in Fig. 2-28.

Nickel ore bodies with a Ni content of more than 10,000 ppm and with a sizable extent are considered to be located in four places, taking account of the assay results of the ore samples obtained on the surface, those of the ore samples from the trenches and pits, and those of the soil







samples for geochemical analysis. Fig. 2-29 shows such places as Gold Hill, Chrome Ridge, Main Ridge and Golf Links.

The Geology of the mineralized zones is as follows.

(a) Gold Hill (surface area: approximately 100,000 m<sup>2</sup>)

The altered nickel-enriched serpentinite containing a large amount of garnierite is exposed on the surface, and the samples for geochemical survey and the ore samples obtained from the surface include those of high nickel grade. This is the mineralized zone showing the most advanced erosion among the four zones.

(b) Golf Links (surface area: approximately 180,000 m<sup>2</sup>).

A very gently inclined flat landform extends on the eastern side and it is considered to correspond to a relic topography of the eroded surface of a peneplain, which has been named "Cherangani plane" (McCall, 1964) from the altitude above sea level. The nickel enrichment zone occurs at a depth more than one meter below the colluvial surface bed, on which an eroded reddish brown soil with an irregular thickness is present, or lacking.

(c) Chrome Ridge (surface area: approximately 100,000 m<sup>2</sup>)

Chromite deposits are contained in the rocks of this area. The topography is a little steeper than that of the Gold Hill. Thin surface soil less than 0.5 meter thick covers the eroded reddish brown soil bed or the nickel-rich altered serpentinite.

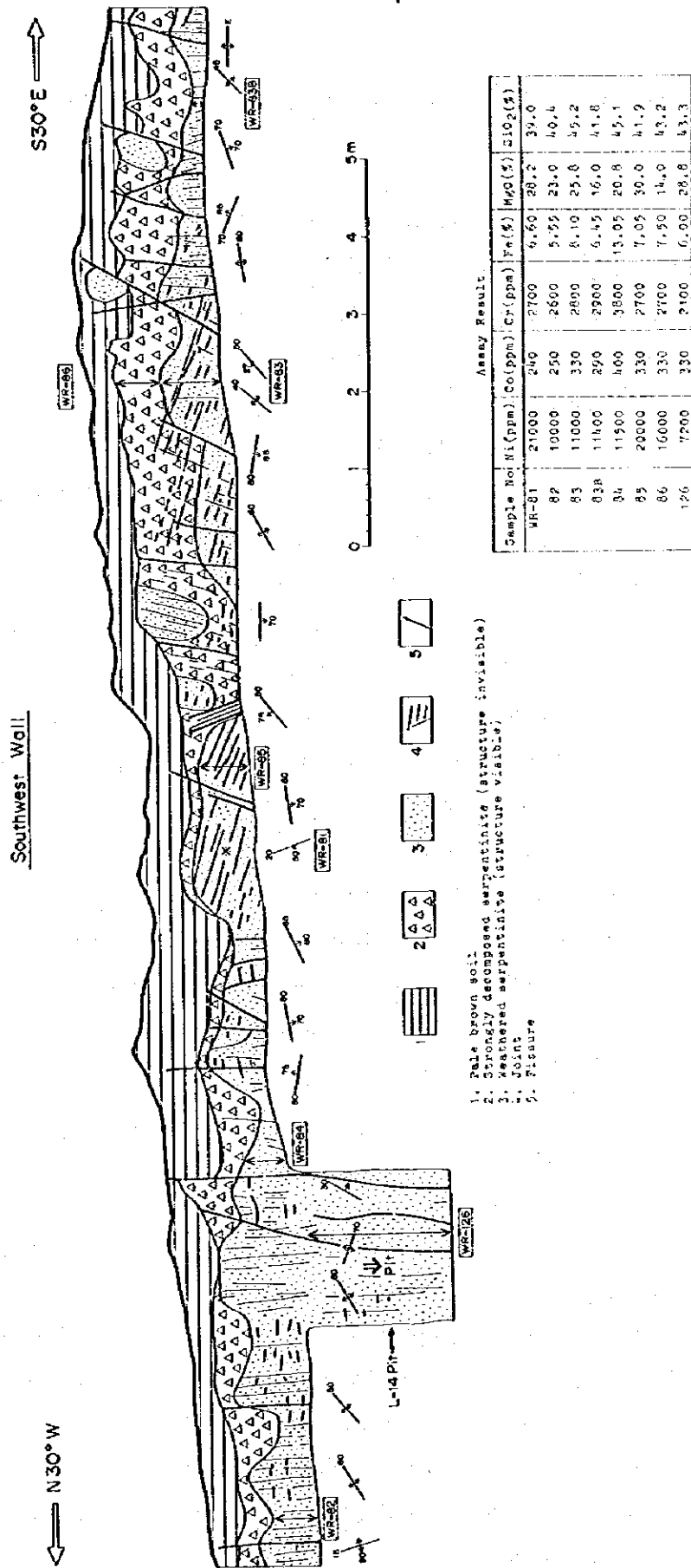
(d) Main Ridge (surface area: approximately 50,000 m<sup>2</sup>).

The landform is a little more gentle than that of the Gold Hills. Weathered serpentinite 0.5 meter thick is distributed underneath the humus soil zone of about 0.5 meter thick. The nickel enriched altered serpentinite occurs below the weathered serpentinite.

The nickel ore in the mineralized zone is classified into the following categories.

- (a) Earthy altered serpentinite
- (b) Blocky weathered serpentinite
- (c) Film-like veinlets and fissure-filling material
- (d) Reddish brown soil
- (e) Dissemination or crust in relatively fresh serpentinite

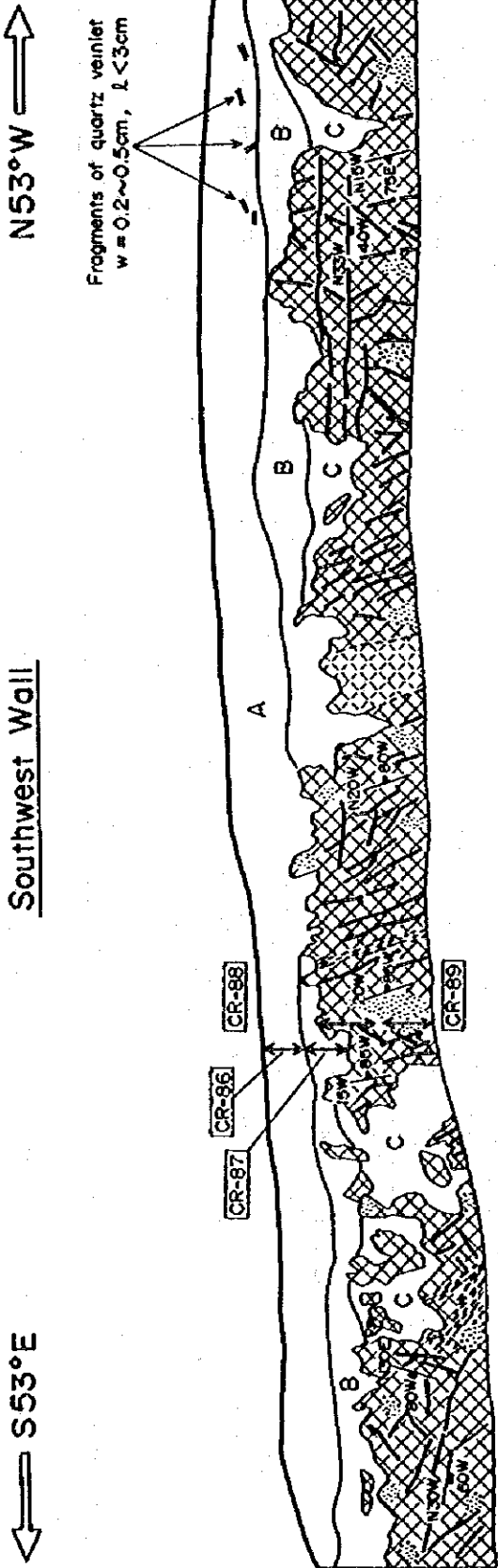
(a) and (b) correspond to the C-horizon of the classification of soil, often showing the values of more than 10,000 ppm Ni, and accompanied by (c) of high-grade in many cases. (d) corresponds to the B-horizon in the classification of the soil profile, and it is a part with a high concentration of iron hydroxide. The nickel grade is 2,500 to 5,000 ppm in general, showing a low grade except for only one sample which showed a value of 8,000 ppm. Although (e) is high in grade locally, but considerably low in bulk.



1. Pale brown soil
2. Strongly decomposed serpentinite (structure invisible)
3. Weathered serpentinite (structure visible)
4. Joint
5. Fracture

Sample No	Ni (ppm)	Co (ppm)	Cr (ppm)	Fe (%)	Mn (%)	SiO <sub>2</sub> (%)
WR-81	21000	240	2700	6.60	20.2	39.0
82	10000	250	2600	5.52	23.0	40.4
83	11000	330	2800	8.10	25.0	39.2
83a	11400	290	2900	6.42	16.0	41.8
34	11500	400	3800	13.02	20.8	45.1
85	20000	330	2700	7.02	30.0	41.9
86	16000	330	2700	7.50	14.0	43.2
126	7200	330	2100	6.00	28.8	43.3

Fig. 2-26 Geological Sketch of L-14 Trench



- Serpentinite
- Silicified serpentinite
- Schist sity
- Joint
- Assayed sample No.

- Garnierite stain along cracks
- Sheared serpentinite
- Cracks in serpentinite

- A. Brown soil (A horizon) with gravels of serpentinite, silicified serpentinite talc schist and chlorite schist
- B. Reddish brown soil (B horizon) with fragments of serpentinite and silicified serpentinite
- C. Brown soil (C horizon?) with fragments of serpentinite and silicified serpentinite

Assay Result

	Ni(ppm)	Co(ppm)	Cr(ppm)	Fe(%)	MgO(%)	SiO <sub>2</sub> (%)
CR-86	4300	680	10000	9.45	21.0	37.7
87	4900	570	4500	9.00	27.2	43.5
88	7400	220	3200	5.40	26.0	48.2
89	9200	440	2900	6.75	14.2	40.2

Fig. 2-27 Geological Sketch of R-18 Trench

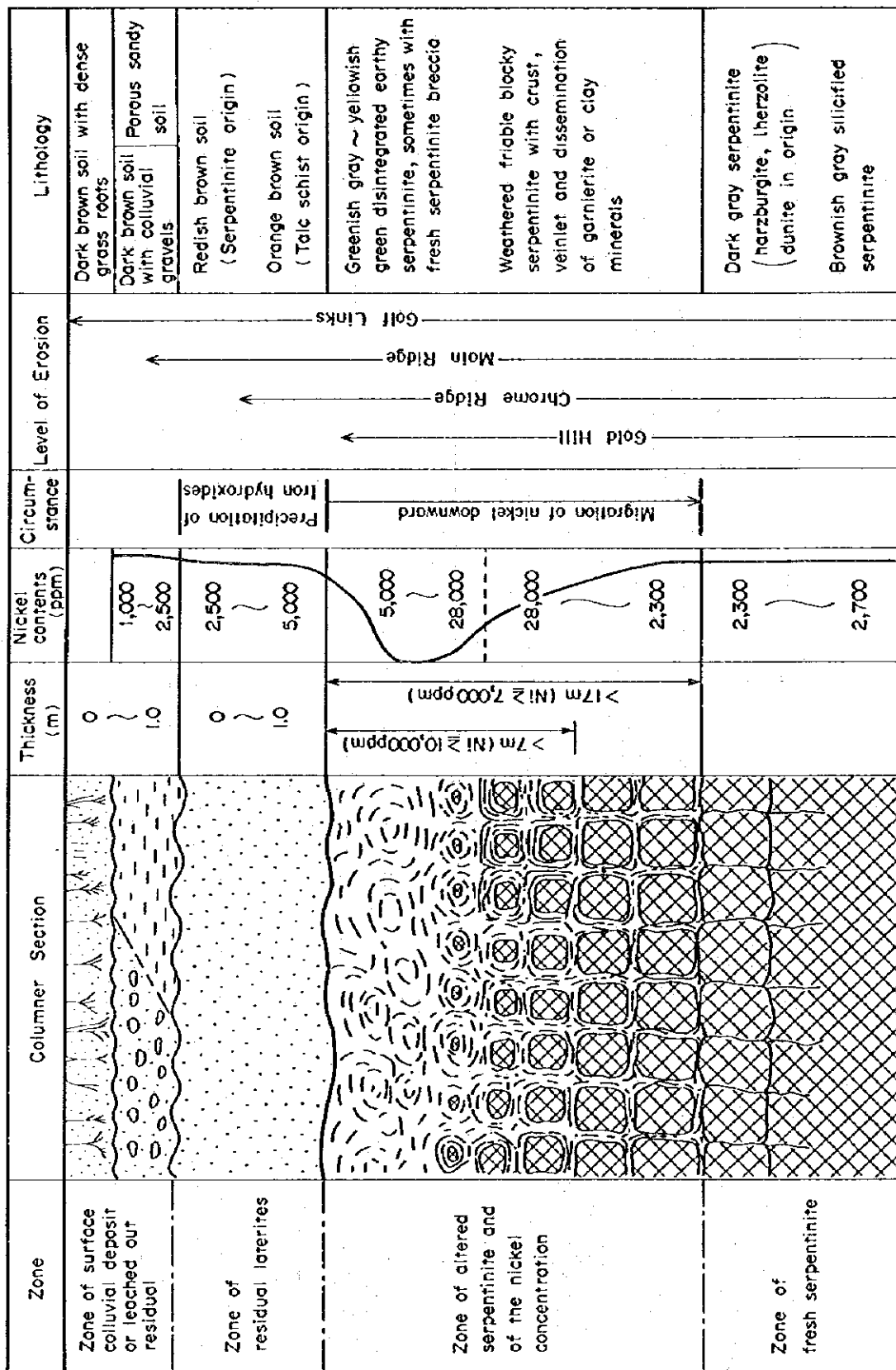


Fig. 2-28 Generalized Profile of Telot Garnierite Deposit





Fig. 2-29 Nickel Ore Bodies and Location of Pits and Trenches

Table 2-17 Result of Chemical Analysis of Nickel Ore

Sample No.	Location <sup>#1</sup>	Depth (m)	Type of Ore (Rock) <sup>#2</sup>	Assay Results						Other Test <sup>#3</sup>
				Ni (ppm)	Co (ppm)	Cr (ppm)	Fe (%)	MgO (%)	SiO <sub>2</sub> (%)	
BR 14	K-13 S	0	Strongly weathered serp. with garnierite	13,000	240	2,200	6.15	32.5	41.2	
81	DD-15 S	0	ditto	10,600	240	1,900	5.25	35.8	40.3	
120	J-20 P	0.6-0.8	Pale brown talc-soil	3,700	330	2,100	6.15	20.8	56.3	
123	K-17 P	0.8-1.1	Reddish brown soil with silicified serp. breccia	4,200	290	4,400	8.55	14.0	56.1	
126	M-20 P	1.1-1.5	Strongly weathered silicified serp.	5,900	270	3,500	8.55	28.8	39.8	
128	P-20 P	0.2-1.0	Strongly weathered talc schist	4,300	250	2,100	6.45	16.6	59.9	
130	J-14 P	1.3-1.5	Khaki soil	4,500	320	2,600	7.95	28.0	45.0	Au-Ag
131	D-14 P	0.3-0.7	Strongly weathered earthy talc schist	3,200	450	4,500	10.65	20.6	47.3	
134	A-12 P	0.8-1.2	Brown soil (talc-schist origin)	6,000	1,020	8,400	16.65	17.4	41.0	
137	V-19 P	0.9-1.3	Reddish brown weathered disintegrated serp.	7,700	240	2,500	6.60	19.8	41.5	
139	S-20 P	0.5-0.8	Yellowish green weathered serp.	9,500	250	2,700	6.60	30.8	42.2	
140	ditto	1.6-1.8	Green yellow strongly weathered serp.	8,000	220	1,900	4.95	24.8	55.6	
CR 40	FF-31 T	0-0.5	Brown porous hard soil, upper zone	2,700	240	3,300	11.25	11.0	43.5	
41	ditto	0.5-1.0	ditto lower zone	2,700	260	2,600	10.25	10.6	43.0	
42	ditto	1.0-1.5	Colluvial & alluvial gravel layer	2,800	220	3,100	8.10	8.3	40.6	
54	BB-26 P	1.2-1.6	Yellowish green strongly weathered serp.	10,900	250	2,200	6.90	26.8	41.0	
64	BB-14 P	0-0.4	Brown porous soil	6,400	270	2,800	10.80	18.0	36.6	
65	ditto	0.4-0.7	Reddish brown soil	7,200	290	2,400	11.40	15.2	37.1	
66	ditto	0.7-1.5	Pale brown & white weathered schistosed serp.	3,500	220	2,000	5.70	13.2	42.7	
82	Y-14 P	0.7-0.8	Reddish brown soil	4,700	420	6,700	14.40	14.6	37.3	
83	ditto	0.8-1.2	Reddish brown soil with serp. breccia	4,600	660	5,600	12.30	28.0	36.7	
84	ditto	1.2-1.5	Light brown soil with serp. breccia	3,900	540	4,100	8.40	28.8	39.0	
85	ditto	1.1-1.5	Weathered serp. with yellow mineral on surface	5,200	210	2,200	4.50	33.0	44.1	X-R
86	R-18 T	0-0.3	Brown surface soil	4,300	680	10,000	9.45	21.0	37.7	
87	ditto	0.3-0.6	Reddish brown soil	4,900	570	4,500	9.00	27.2	43.5	
88	ditto	0.4-0.9	Weathered yellowish green serp.	7,400	220	3,200	5.40	26.0	48.2	
89	ditto	0.9-1.3	ditto	9,200	450	2,900	6.75	14.2	40.2	
WR 18	L-15 S	0	Pale green weathered serp.	9,000	190	2,200	5.40	31.0	41.1	
19	L-13 S	0	Dark gray weathered serp.	4,300	450	2,200	5.25	25.2	40.7	
41	O-12 S	0	Gray fresh serp.	2,700	190	1,500	4.50	31.6	39.6	X-R
46	O-15 S	0	Weathered yellowish green serp.	9,100	460	1,900	5.55	34.8	41.8	
81	L-14 T	1.0	Strongly weathered garnierite rich serp.	21,000	240	2,700	6.60	28.2	39.0	X-R
82	ditto	0.8-1.4	Yellowish green weathered serp.	10,000	250	2,600	5.55	23.0	40.4	
83	ditto	0.9-1.7	ditto	11,000	330	2,800	8.10	25.8	45.2	X-R
83B	ditto	1.2-1.4	ditto	11,400	290	2,900	6.45	16.0	41.8	
84	ditto	1.0-1.6	ditto	11,500	400	3,800	13.05	20.8	45.1	
85	ditto	0.6-1.3	Strongly weathered garnierite rich serp.	20,000	330	2,700	7.05	30.0	41.9	
86	ditto	0.3-0.9	Greenish grey strongly weathered earthy serp.	16,000	330	2,700	7.50	14.0	43.2	
113	M-8 P	0.8-1.1	Light orange brown soil	4,100	400	4,700	12.00	10.8	40.5	
114	P-10 P	0.5-0.9	Weathered silicified serpentinite	2,700	280	3,200	6.45	31.8	40.0	
115	ditto	0.9-1.6	Weathered serp. with yellowish green mineral	5,000	300	2,400	6.15	14.2	40.6	
119	P-14 P	1.4-1.7	Pale grey silicified schistosed serp.	2,400	260	1,100	3.00	33.4	49.6	
121	L-11 P	1.2	Grey weakly weathered serp.	4,600	260	1,400	3.75	37.6	42.4	
122	ditto	1.0-1.6	Weathered greenish brown serp.	9,400	340	2,300	7.35	38.0	38.0	
123	ditto	0.6-1.0	Strongly weathered orange brown serp.	13,200	390	3,600	8.40	31.4	39.5	
124	ditto	0.4-0.6	Decomposed bleached serp.	2,300	240	1,500	3.15	36.0	43.1	
126	L-14 P	2.1-3.6	Strongly weathered pale greenish grey serp.	7,200	330	2,100	6.00	28.8	43.3	X-R
131	V-14 P	1.1-1.6	Weathered, disintegrated serp.	2,900	270	4,000	4.80	23.6	42.9	
176	O-21 S	0	Fresh serpentinite	2,400	310	1,700	4.50	36.4	35.1	
182	K-13-14 S	0	Greenish brown weathered earthy serp.	9,000	480	4,000	10.35	26.0	42.8	Au-Ag X-R

#1 P: Pit, T: Trench, S: Surface, Ref: Plate .....

#2 Serp.: serpentinite

#3 Au-Ag: Chemical Analysis for Au and Ag, X-R: X-ray diffractive analysis, IS: Thin section

The nickel ores consist of antigorite or garnierite, montmorillonite, chromite and quartz. The veinlet-like green part contains illite and illite-montmorillonite mixed-layer minerals. It is very difficult to distinguish antigorite from garnierite by X-ray diffraction, but it is likely that these samples consist mainly of antigorite, being accompanied by garnierite, or they are composed of garnierite with low nickel content judging from the assay values of the samples (Ni: 7,000 to 21,000 ppm).

The ore samples taken from three ore bodies i.e. Gold Hill, Chrome Ridge and Golf Links which show good exposure of mineralized zone were used for calculation of the average grade. The result is shown in Table 2-17, 2-18.

Table 2-18 Average Grade of Nickel Ore Bodies

Ore Body	Contents	Ni (ppm)	Co (ppm)	Cr (ppm)	Fe (%)	MgO (%)	SiO <sub>2</sub> (%)
Gold Hill		10,600	340	2,600	6.94	30.0	41.6
Chrome Ridge		7,900	290	3,000	6.48	23.4	44.8
Golf Links		7,000	320	3,000	8.15	25.8	39.4
Average		8,500	320	2,900	7.19	26.5	41.9

Among these three ore bodies, the Gold Hill ore body has the highest nickel grade while the other two are relatively low. This is likely to be due to the fact that enrichment zone is exposed on the Gold Hill area, whereas overburden is relatively thick at other bodies, having led to less frequency of taking samples of the nickel enriched part lower.

However, the nickel grade in the two ore bodies is estimated to be about 10,000 ppm and is similar to that of Gold Hill when referring to the results of trenching in the past, and it is considered that the grade will be Ni + Co = 1.1% approximately in all the three ore bodies. This value is fairly low as compared with the grade (Ni + Co > 2.0%) of nickel deposits of the same type in operation in other parts of the world.

For calculation of ore reserves, any basis for further revision of the results of calculation of ore reserve performed by the Department of Mines and Geology who revised the calculation conducted earlier by the New Consolidated Gold Fields Ltd., was not found.

The assumption of the depth by the Department of Mines and Geology was based on the results of drilling, which is considered to be accurate to a considerable extent. Further, the extent of mineralized zone and the area set up are almost the same as those obtained in the current

survey. It can be said, therefore, that the calculation of the ore reserves by the Department of Mines and Geology might be reasonable. However, because the topography of the mineralized zone is fairly steep and because the mineralized zone would not always show a regular zonal arrangement from the evidences observed in the pits and trenches, more investigation would be required for a more accurate calculation of ore reserve and grade.

### (3) Gold

As a result of geological survey along the survey lines set up for geochemical prospecting, it became clear that the area of mining is within the silicified zone, that the silicified zone shows a remarkable extension in the direction of north to south, and that the main part is at the central part of the serpentinite body with a width of up to 350 meters (Fig. 2-31).

Mining work of gold led to a conclusion that soils containing fine-grained siliceous materials was relatively high in gold content. It was therefore concluded that the gold mineralization is related to silicification.

As a result of observation and examination of trenches (Fig. 2-30) and pits, and the surface geological survey, siliceous materials in the silicified zone are divided into chalcedonic quartz vein, white quartz vein, silicified serpentinite and silicified talc schist.

Laboratory tests comprising chemical analysis, microscopy of polished section and X-ray diffraction revealed that chalcedonic quartz is the silicified material to be related to the mineralization of gold and silver.

#### Discussion on Mineralization

It is an important fact that the gold mineralization at Telot is closely related to the silicified parts of serpentinite and talc schist, that the main part of the silicified zone continues for two kilometers northwards with a width of about 350 meters, and that most of the samples with geochemically anomalous values of gold described later (2-4-3) are contained in the zone with 350 meter width.

According to the result of geological survey, the distribution of lenticular talc schist is often observed within fractured parts in serpentinite and along faults.

On the other hand, occurrence of talc schist is often observed, and at the same time, strong silicification is also observed in pits and trenches excavated in the silicified zone in the central part (e.g. M-16 trench, Fig. 2-30).

It seems therefore that the silicified zone includes a series of faults and fractured zones, suggesting that gold mineralization associated with silicification took place through the faults and the fracture zones.

Since both the gold deposit of Telot and the gold deposit found in the upper reaches of the

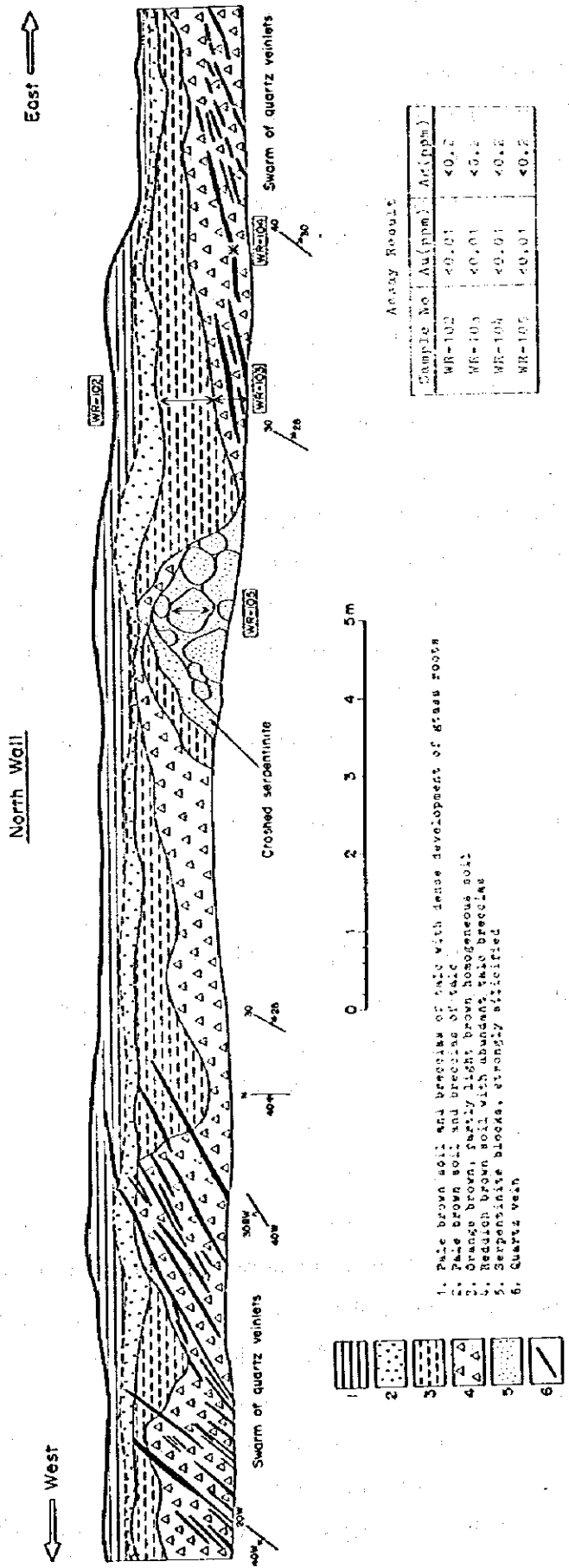


Fig. 2-30 Geological Sketch of M-16 Trench

Endogh River (report of the first year) are emplaced in serpentinite or talc schist accompanied with the ultrabasic rock, and taking into account that both deposits are contained in the same tectonic zone, it can be interpreted that the primary gold which had been contained in the ultrabasic rock might be concentrated by the effect of tectonic movement in the formation of Telot gold deposit.

#### Ore Reserves and Grade

Ore reserves is to be calculated on the assumption that open pit method is applied for mining operation. Supposing that the mineralized zone occupies a maximum extent in the silicified zone shown by the gold content above the detection limit of geochemical samples, the area is 350 m x 2,000 m = 700,000 m<sup>2</sup>.

If it is assumed that the depth of the weathered zone which is easy to mine is 4 meters and that the specific gravity of ore is 2.5, the ore reserve is 700,000 m<sup>2</sup> x 4 m x 2.5 = 7,000,000 tons.

The grade is estimated to be about one gramme per ton at the high grade part. However, average grade for the whole reserve is considered to be considerably lower than 0.5 gramme per ton taking the result of geochemical prospecting into consideration. This is fairly low as compared with the average grade of the operating open pit mines in the world, which is 0.1 oz/ton = 3 gr/ton.

Therefore it is considered that the deposit is not suitable for systematic open pit mining.

#### 2-4-3 Geochemical Survey

The area of detailed geochemical survey, 3 km<sup>2</sup>, is included in the detailed geological survey area, covering the Telot serpentinite body in which chromite, garnierite and eluvial gold deposits occur. The area was selected for follow-up in order to evaluate the gold, chromium and nickel mineralizations. For this purpose, a grid system with 100 m by 50 m unit was designed, and 607 soil samples were collected for analysis of Au, Ni and Cr.

##### (1) Statistic Value, Distribution and Data Processing

Table 2-19 lists the statistic values of analytical elements. Mean and standard deviation of Au are not calculated because analytical results of Au are mostly under the detection limit. Table 2-20 and 2-21 show the statistic values for Cr and Ni classified according to parent rocks of soil samples such as all serpentinite, non-silicified serpentinite, silicified serpentinite, talc schist and amphibole schist (including chlorite schist and hornblende gneiss).

Cumulative frequency distribution curves for the elements are shown in Fig. 2-32. Analytical values over detection limits were used for the figures.

Fig. 2-33 and 2-34 give cumulative frequency distribution curves for Cr and Ni classified



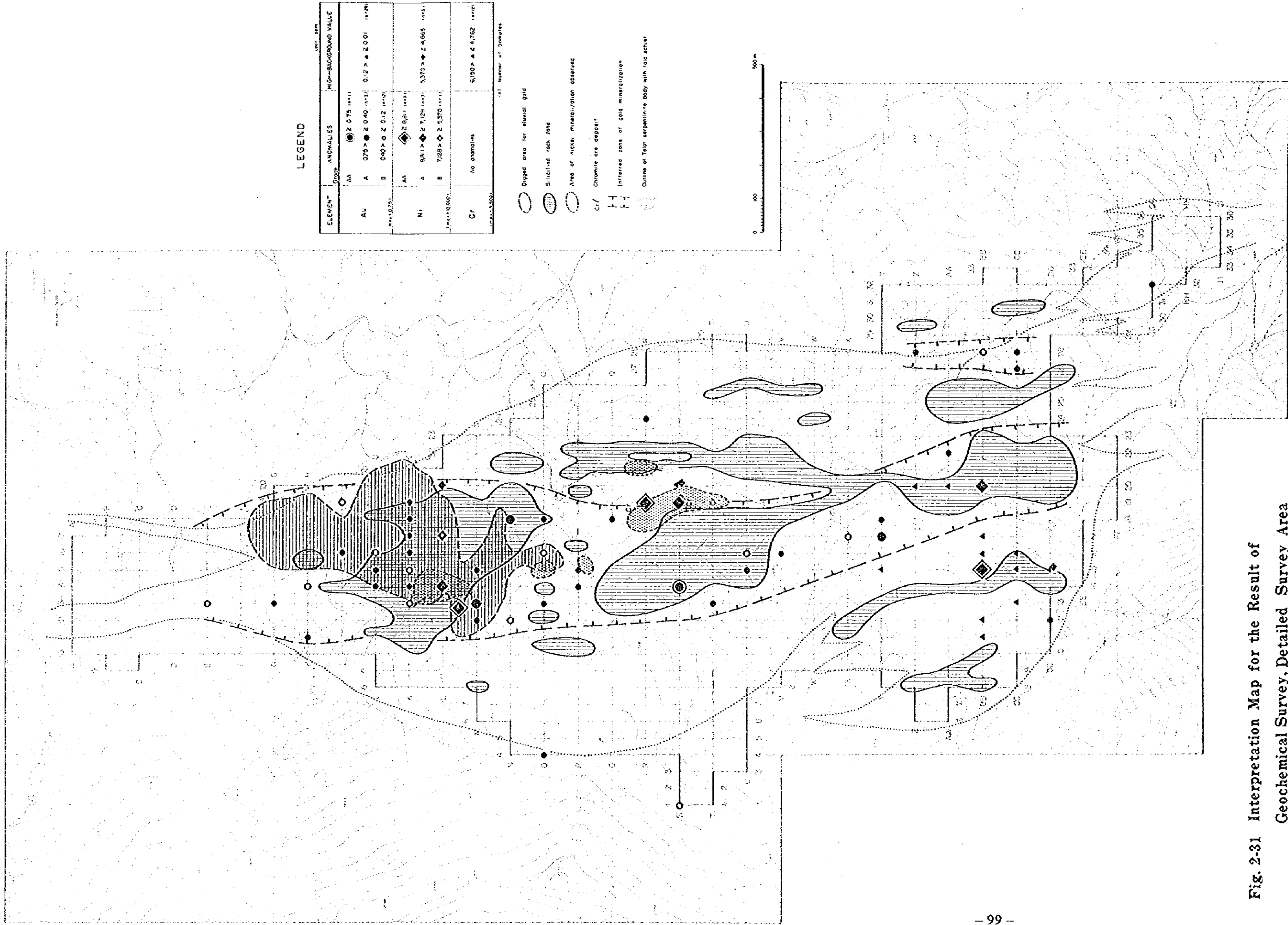


Fig. 2-31 Interpretation Map for the Result of Geochemical Survey, Detailed Survey Area





Table 2-19 Statistic Values of Analyzed Elements, Detailed Survey Area

Element Unit	Cr ppm	Ni ppm	Au ppm
Number of Samples	607	607	607
Number of Samples Under Detection Limit	0	0	562
Maximum Value	5,500	10,000	0.75
Minimum Value	40	60	<0.01
Mean ( $\bar{x}$ )	1,515	1,624	-
Standard Deviation (S.D. in Log figure)	0.373	0.401	-
$\bar{x} + 2$ S.D.	8,451	10,308	-

Table 2-20 Statistic Values of Cr by Parent Rocks, Detailed Survey Area

Unit: ppm

Parent Rock	Serpentinite (All)	No-Silicified Serpentinite	Silicified Serpentinite	Talc Schist	Amphibole Schist
Number of Samples	323	133	140	72	88
Maximum Value	5,500	5,170	5,250	3,990	2,640
Minimum Value	100	100	400	480	40
Mean ( $\bar{x}$ )	2,210	2,045	2,200	1,554	458
Standard Deviation (S.D. in Log figure)	0.222	0.267	0.168	0.216	0.383
$\bar{x} + 2$ S.D.	6,148	6,990	4,765	4,194	2,672

Table 2-21 Statistic Values of Ni by Parent Rocks, Detailed Survey Area

Unit: ppm

Parent Rock	Serpentinite (All)	No-silicified Serpentinite	Silicified Serpentinite	Talc Schist	Amphibole Schist
Number of Samples	323	133	140	72	88
Maximum Value	10,000	9,000	8,400	3,460	3,380
Minimum Value	160	160	520	270	60
Mean ( $\bar{x}$ )	2,469	2,198	2,592	1,948	392
Standard Deviation (S.D. in Log figure)	0.184	0.204	0.152	0.208	0.450
$\bar{x} + 2$ S.D.	5,765	5,621	5,228	5,088	3,121

Table 2-22 Correlation Coefficients, Detailed Survey Area

	Cr	Ni	Au
Cr			
Ni	0.879 (607)		
Au	0.095 (45)	0.091 (45)	

R( $\phi, e$ )  
 $\phi$ : degree of freedom  
 $e$ : significance level

IRI (43,0.01) = 0.380  
 IRI (605,0.01) = 0.104

( ) Number of paired samples calculated

Table 2-23 Correlation Coefficients between Cr and Ni by Parent Rocks, Detailed Survey Area

	Serpentinite (All)	No-silicified Serpentinite	Silicified Serpentinite	Talc Schist	Amphibole Schist
Correlation Coefficient (Cr-Ni)	0.636 (323)	0.770 (133)	0.449 (140)	0.779 (72)	0.852 (88)

( ) Number of paired samples calculated

R( $\phi, e$ )  
 $\phi$ : degree of freedom  
 $e$ : significance level

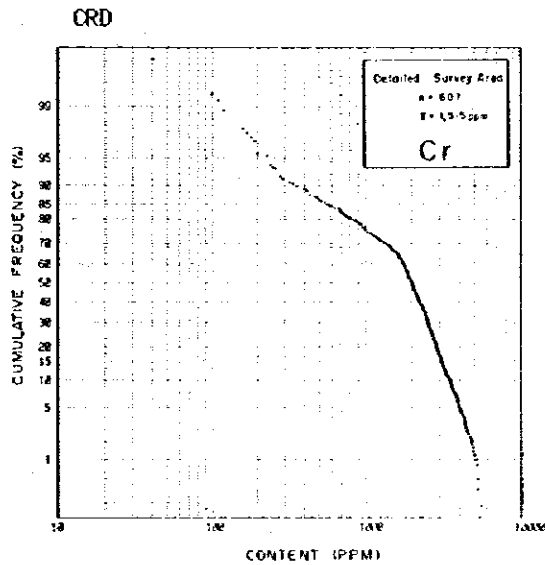
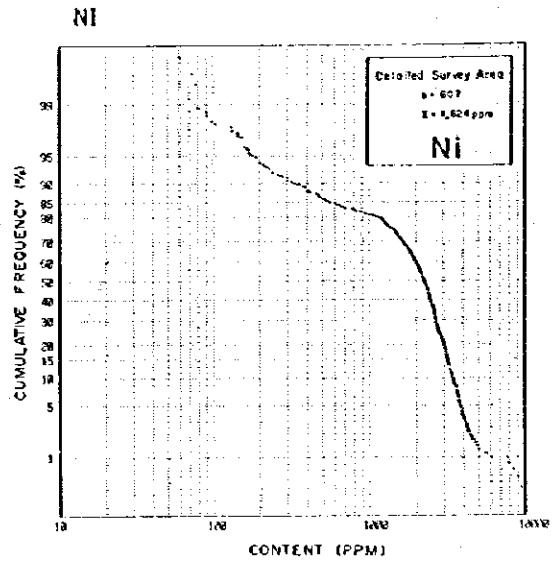
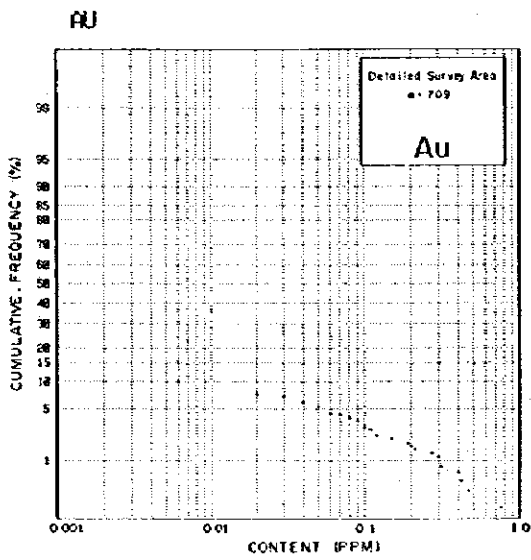
IRI (70,0.01) = 0.302    IRI (86,0.01) = 0.273  
 IRI (131,0.01) = 0.223    IRI (138,0.01) = 0.217  
 IRI (321,0.01) = 0.143

Table 2-24 Thresholds and Classification of Anomalous Values, Detailed Survey Area

Unit: ppm

Element	Anomalies			Threshold	High-background Value
	Grade AA	Grade A	Grade B		
Cr	-	-	-	6,150	6,150 > Cr $\geq$ 4,762 (12)
Ni	Ni > 8,811 (3)	8,811 > Ni $\geq$ 7,128 (3)	7,128 > Ni $\geq$ 5,370 (1)	5,370	5,370 > Ni $\geq$ 4,665 (3)
Au	Au $\geq$ 0.75 (1)	0.75 > Au $\geq$ 0.40 (3)	0.40 > Au $\geq$ 0.12 (12)	0.12	0.12 > Au $\geq$ 0.01 (29)

( ) Number of samples



**Fig. 2-32 Cumulative Frequency Distribution Diagrams for Analytical Elements, Detailed Survey Area**

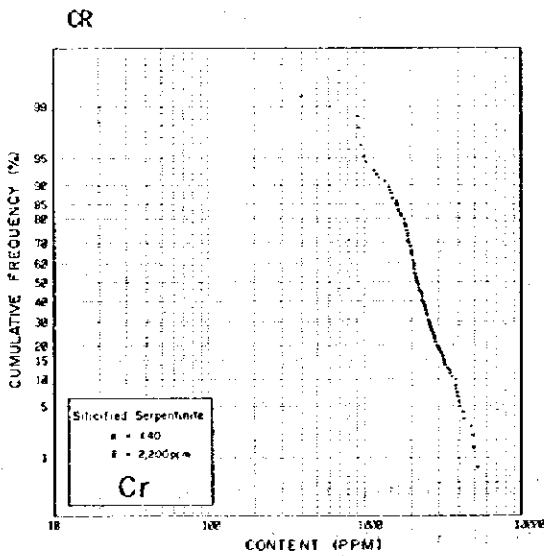
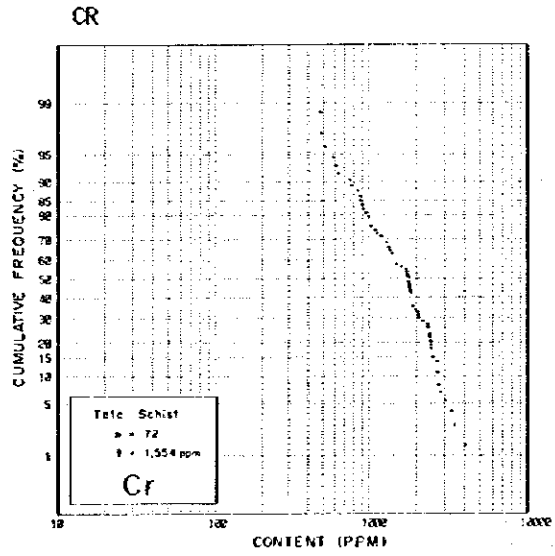
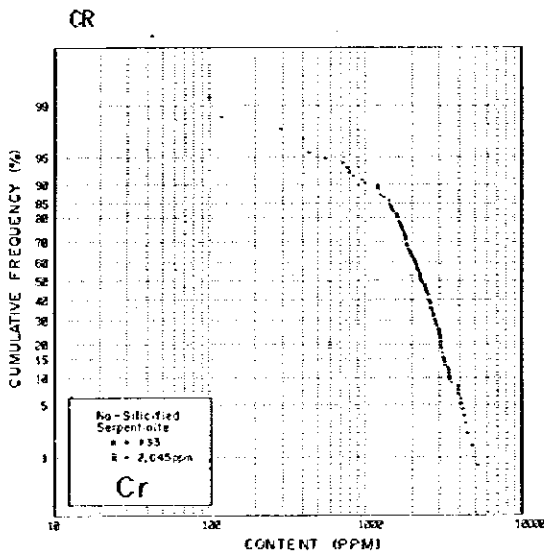
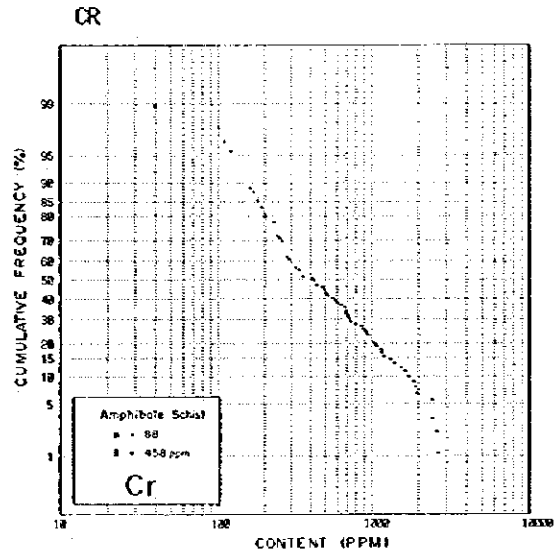
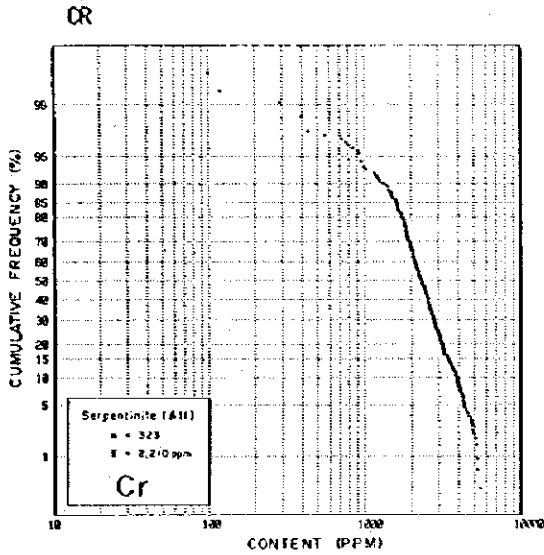
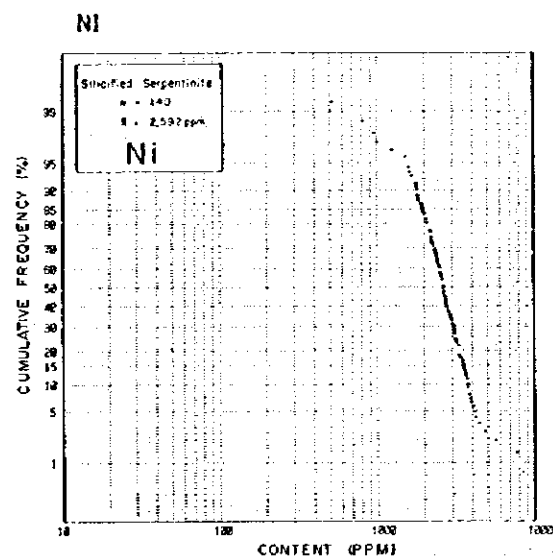
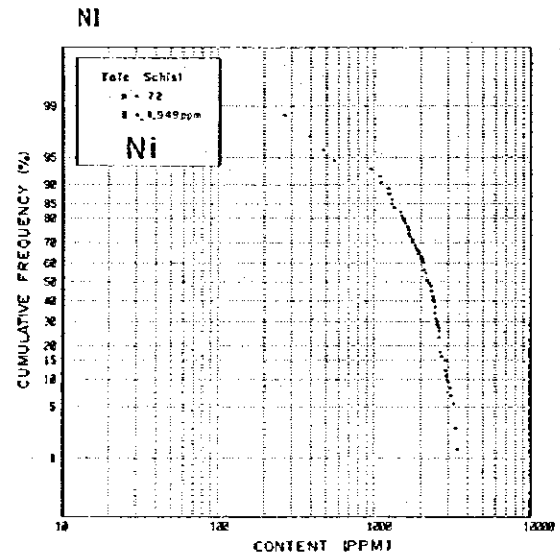
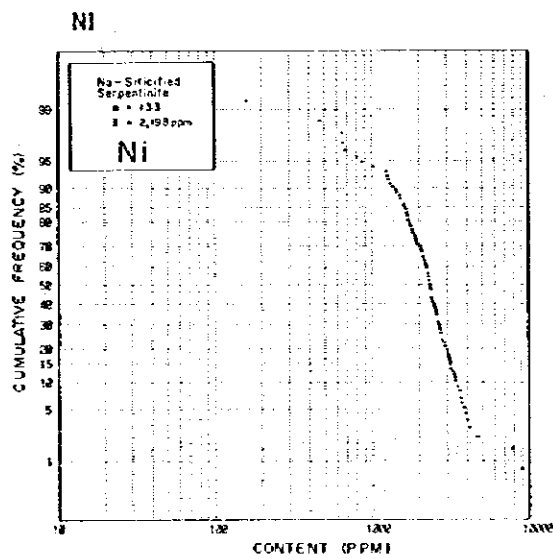
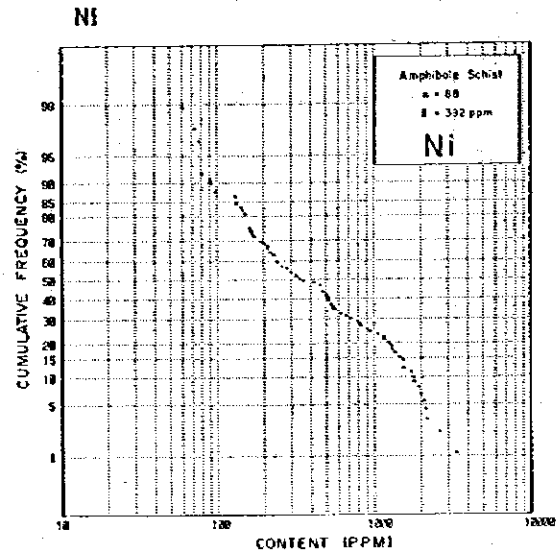
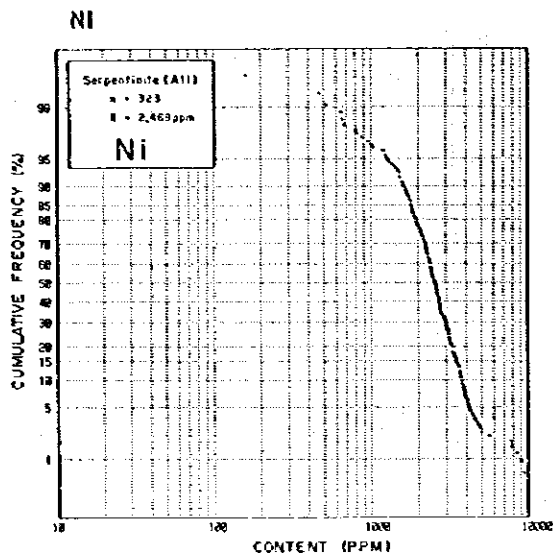


Fig. 2-33 Cumulative Frequency Distribution Diagrams for Cr by Parent Rocks, Detailed Survey Area



**Fig. 2-34 Cumulative Frequency Distribution Diagrams for Ni by Parent Rocks, Detailed Survey Area**

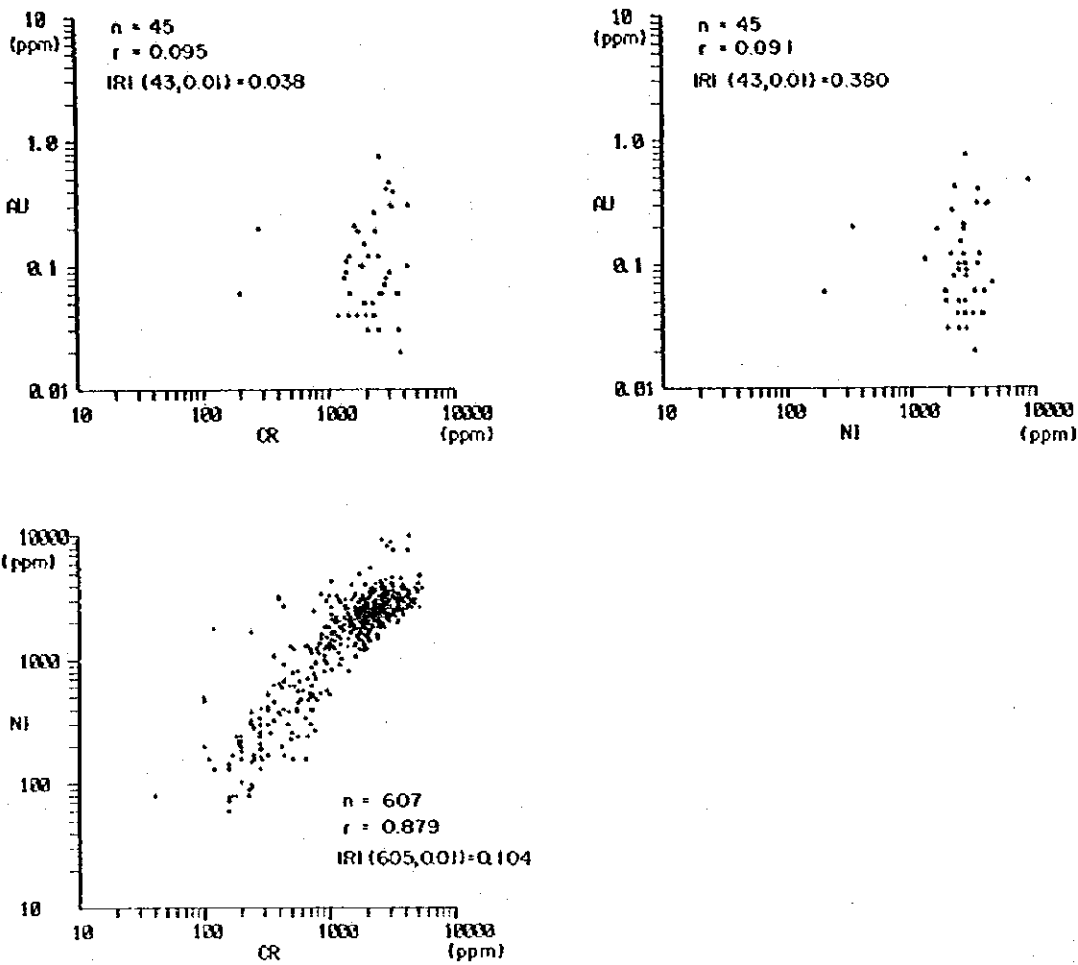


Fig. 2-35 Scatter Diagrams, Detailed Survey Area

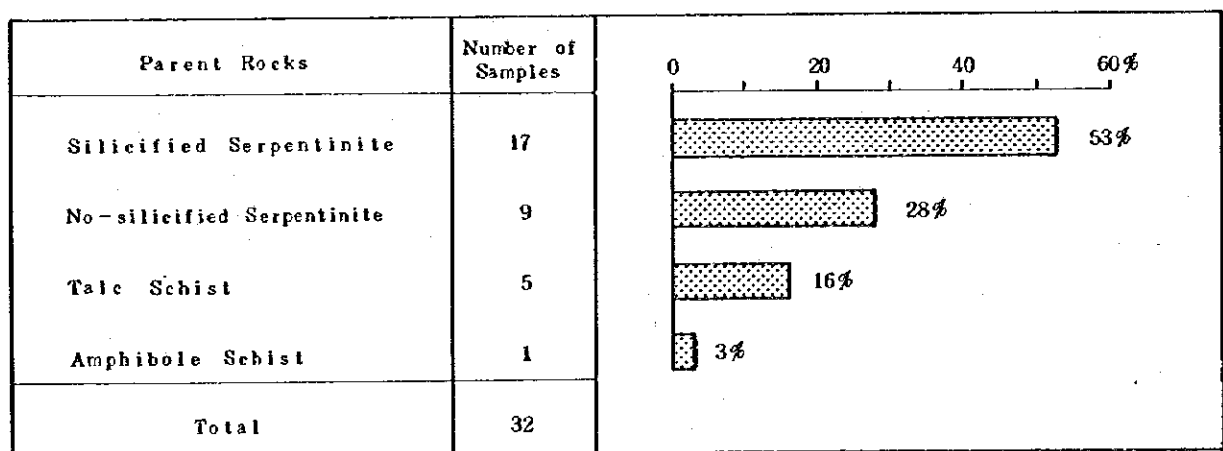


Fig. 2-36 Histogram for Parent Rocks of Soil Samples with Gold Content over Detection Limit, Detailed Survey Area

according to parent rocks mentioned above.

Table 2-22 and 2-23 give the correlation coefficients for the elements and |R| values of significance test. Analytical values over detection limits were used for the calculation and the numbers of paired samples calculated are written under each correlation coefficient.

Threshold values and anomalous values of each elements are shown in Table 2-24.

## (2) Interpretation of Geochemical Anomalies

Fig. 2-31 shows the distribution of anomalous and high-background value samples, the excavated area for eluvial gold, silicified serpentinite, chromite and garnierite occurrences and the inferred zone of gold mineralization.

The followings are the interpretation of geochemical anomalies for each element.

### (a) Cr

No anomalous samples are extracted.

All high-background value samples (Cr: 4,800-5,500 ppm) except one sample are in the Golf Links area, and further eight samples are concentrated around the point CC-15. However, no occurrence of chromite has been noted in the area. On the contrary, only one high-background value sample (Cr: 5280 ppm) was obtained in the area where chromite ore bodies and floats are distributed. The fact may be explained as follows: the resistivity of chromite to weathering is so strong that very few grains of chromite under 80 mesh are produced, resulting in rare appearance of Cr anomaly.

It seems that the concentrical distribution of high-background values in Golf Links area is caused by the residual soil of serpentinite containing much chromium.

### (b) Ni

Two each of AA-grade and A-grade anomalous samples (Ni: 7,800-9,400 ppm) are in or near the known mineralized area of garnierite, showing good relationship between them. Other three anomalous samples (Ni: 5,600-10,000 ppm) are distributed separately and the feature possibly means local concentration of Ni near the surface.

Nickel mineralization in deeper zone, under the depth of about 50 cm, was not detected during the geochemical survey because the depth of soil samples was limited to shallow surface zone. Consequently evaluation of nickel mineralization is difficult and can not be done using the result of geochemical survey only. It should be done by adding the data from pits, trenches, shallow drilling etc.

### (c) Au

Many anomalous samples (Au: 0.12-0.75 ppm) and high-background value samples are distinctly distributed in a zone trending N-S. The anomalous zone is almost bordered by the E and



Y survey lines and by the No. 12 and No. 19 survey lines with a length of 2,000 m in the N-S direction and the width of 350 m in the E-W direction. 88% of the total number of the anomalous samples and 69% of high-background value samples are within this zone. Further, 50% of anomalous samples and 41% of high-background value samples are distributed in the northern half of the zone bordered by the I and O survey lines with a length of 600 m in the N-S direction. About one-third of the soil samples show gold content over detection limit in the northern half of the zone. It shows a good relationship between the results of geochemical survey and geological survey and the area dug for eluvial gold is entirely included in the northern half of the zone.

Fig. 2-36 shows mutual relationship between gold mineralization and silicification observed mainly in serpentinite. The parent rock constituting 53% of the samples with gold content over detection limit is silicified serpentinite.

The anomalous zone and silicified serpentinite zones are mostly included in the central zone of the Telot serpentinite body trending in the N-S direction. Large and strongly silicified zones are particularly distributed in the anomalous zone.

In conclusion, new productive area for eluvial gold can be expected in the southern half of the anomalous zone judging from the distribution of anomalous samples, high-background value samples, silicified zones and the excavated area for eluvial gold.

## 2-5 Area C (Geophysical Survey)

### 2-5-1 Outline of Survey

The airborne geophysical survey in the KVDA area conducted by Mines and Geological Department under European Community aid revealed two pronounced high magnetic bodies in the northeast part of the project area. If these magnetic bodies are proved to be serpentinites, they may have high potential for chromium mineralization taking into account that the Telot serpentinite body which is situated to the southwest of the bodies has chromite bodies and showed same magnetic response.

Hence ground geophysical survey comprising gravity and magnetic surveys was designed for the area of sixty square kilometers, which covers two magnetic bodies, to clarify the potentiality of chromite deposits.

Table 2-25 and Table 2-26 show the outline of survey and the number of samples used for laboratory test respectively.

Table 2-25 Outline of Geophysical Survey

Method	Outline of Works	
Gravity Survey	Area covered	: 60 km <sup>2</sup>
	Length of surveyed line	: 210 km
	Station	: 1100 points
	Station interval	: 200 m
	Leveling	: 1100 points
Magnetic Survey	Area covered	: 60 km <sup>2</sup>
	Length of surveyed line	: 210 km
	Station	: 2155 points
	Station interval	: 100 m

Table 2-26 Laboratory Works Carried Out

Item	Amounts
Magnetic susceptibility	50
Density	50

Fifty six survey lines each four kilometers long were set crossing almost the general geological trend of the area. The observation stations were located at an interval of 100 meters, and

1,100 stations with an interval of 200 meters for gravity survey and 2,155 stations with an interval of 100 meters for magnetic survey were designed respectively.

The position of survey lines and stations was designed using the topographic map of 1:10,000 in scale produced from the aerial photographs.

La Coste and Romberg G-206 type gravimeter was used for gravity prospecting and Scintrex MP-2 type proton magnetometer was used for magnetic prospecting.

### 2-5-2 Geology

The surveyed area, which is situated on the western margin of the Rift Valley, forms a flatland dipping gently to the east, and is covered by alluvial and talus deposits. On the western margin of the area, foliated granites which are one of the basal rocks in the area are exposed and separated from the major parts of the area by a series of the Rift Valley faults. On the northwest part, on the other hand, silicified and brecciated rocks occur in form of veins, and this is thought to be caused by the Rift Valley volcanism. The float zones of basalt which is also considered to be due to the volcanism are observed in the northeast part of the area.

### 2-5-3 Gravity Survey

#### (1) Results of Survey

Gravitational distribution of survey area is explained on the Bouguer map (Fig. 2-37,  $\rho = 2.60 \text{ g/cm}^3$ ) which is considered to reflect very well the geologic structure of the area.

The Bouguer anomalies in the survey area are distributed with a low of  $-142 \text{ mgal}$  in the southern corner to a high of  $-122 \text{ mgal}$  in the northern part showing a total relief of  $20 \text{ mgal}$ .

The distribution of Bouguer anomaly is as follows:

- (a) the gravity contour flows northeastward strongly reflecting the geologic structure of northeasterly trend thought to be present in the survey area, and the gravity decreases sharply from the northwestern part toward the southeast.
- (b) low gravity anomaly is formed in the central part of the survey area, showing an appearance to reflect the basin structure of the basement of the neighboring area, but it becomes indistinct on the northern side of the survey line No. 15, and
- (c) Apart from the above, the gravity contours shift to east-west direction, leading to an estimation of the change of the basement structure in this part.

In the zone of steep inclination of gravity in the northwestern part of the survey area, gravity contours are strongly inclined southeastward with 5 to 10 milligals per kilometer. It is thought that this reflects southeastward steep-dipping of high-density basement in a general.

Table 2-27 Density and Susceptibility of Rock Samples

Group	Sample No.	Rock Name	Location	Density (g/cm <sup>3</sup> )			Susceptibility (x10 <sup>6</sup> cgs-emu)	
				Dry	Wet	Average	emu/cm <sup>3</sup>	Average
Siliceous Dikes	1	Silicified brecciated rock	0/50	2.65	2.66	2.55 (2.57)	60.9	235.7
	2	"	23/32	2.52	2.53		232.2	
	3	"	9/42	2.49	2.52		414.0	
Basalts	4	Basalt	5/11	2.83	2.84	2.80 (2.82)	402.2	435.5
	5	"	3/13	2.81	2.82		682.3	
	6	"	"	2.80	2.82		774.0	
	7	"	3/10	2.81	2.83		386.3	
	8	"	2/13	2.81	2.83		598.5	
	9	"	2/7	2.80	2.82		231.0	
	10	"	2/9	2.76	2.79		198.6	
11	"	4/4	2.78	2.80	211.2			
Gabbros	12	Gabbro	Wakorr	2.96	2.97	2.94 (2.95)	211.2	197.1
	13	"	"	2.91	2.92		183.0	
Serpentinities	14	Serpentinite	Telot	2.78	2.79	2.69 (2.71)	5,401.3	4,532.6
	15	"	"	2.69	2.70		4,816.4	
	16	"	"	2.58	2.59		3,122.1	
	17	Silicified serpentinite	"	2.61	2.63		4,175.4	
18	Talc rock	"	2.81	2.83	5,147.6			
Chromite Ores	19	Chromite ore	"	3.85	3.87	3.84 (3.86)	259.9	382.8
	20	"	"	3.83	3.85		505.6	
Foliated granites	21	Granite	14/41	2.46	2.51	2.52 (2.54)	101.8	202.5
	22	"	10/44	2.54	2.56		221.0	
	23	"	Wakorr	2.59	2.60		310.0	
	24	"	?	2.52	2.55		54.6	
	25	"	22/40	2.55	2.57		144.1	
	26	"	22/41	2.49	2.52		159.4	
	27	"	?	2.51	2.55		722.1	
	28	"	52/34	2.59	2.60		167.2	
	29	"	23/36	2.56	2.58		47.6	
	30	"	23/35	2.49	2.52		157.2	
	31	"	24/39	2.52	2.55		113.9	
	32	"	53/32	2.54	2.57		24.1	
	33	"	21/40	2.50	2.54		74.0	
	34	"	52/30	2.56	2.58		144.1	
35	"	48/38	2.57	2.59	170.8			
36	"	12/34	2.44	2.47	301.3			
37	Silicified granite	9/37	2.48	2.50	227.5			
38	"	9/38	2.39	2.42	397.8			
39	"	11/40	2.49	2.52	309.9			
Basic schists	40	Hornblend-chlorite schist	Telot	2.87	2.89	2.81 (2.84)	190.2	121.3
	41	Chlorite schist	"	2.72	2.75		62.5	
	42	"	"	2.84	2.87		111.2	
Siliceous schists	43	Muscovite-quartz schist	Turkwel Gorge	2.55	2.58	2.57 (2.60)	333.9	321.1
	44	"	"	2.56	2.59		402.7	
	45	Quartz schist	Telot	2.60	2.62		226.7	
Hornblend gneisses (Amphibolites)	46	Hornblend gneiss	Just NW to the Area	3.11	3.13	3.07 (3.08)	115.1	183.3
	47	"	"	3.19	3.20		256.6	
	48	"	26/42	3.06	3.06		269.5	
	49	"	Turkwel Gorge	3.12	3.14		223.3	
50	"	Telot	2.86	2.89	52.1			
Biotite gneisses	51	Biotite gneiss	"	2.60	2.61	2.79 (2.81)	231.2	285.2
	52	"	20/41	3.01	3.03		261.3	
	53	"	Old Road (Orwa)	2.82	2.83		193.6	
	54	"	Turkwel Gorge	2.84	2.86		392.1	
	55	"	Orwa	2.69	2.70		347.7	
Average				2.69	2.71	2.70	683.9	

( ) wet

However, it is a general tendency of the surrounding area that gravity decreases toward the east, and it is also presumed that geologic structure would change in the deeper subsurface. It would be required to take into consideration these. However, the extent of the survey area was too narrow to clarify the above fact during the survey.

It is also assumed that in the steep dipping zone, that the basement subsided by forming a fault, and that the part with the steep inclination of gravity contour may correspond to it. Therefore, it appears that those parts such as from No. 40 of the survey line 9 to No. 38 of the line 20 and from No. 38 of the line 13 to No. 28 of the line 36 would correspond to it. The direction of the zone of steep inclination tends to shift to the northeast in the northern part of the survey area and to the south in the southwestern part, indicating that the basement structure would change to each direction.

The gravity anomaly at the central part of the survey area shows a narrow and long low gravity zone of one to two kilometers wide and more than ten kilometers long being opened toward the southwest, in which gravity tends to decrease gradually toward the southwest.

## (2) Results of Analysis

The density distribution of the rocks in the area requires to be made clear to some extent by means of drilling etc. in order to analyze quantitatively the subsurface structure from gravity distribution. Although the basement rocks are exposed in the western part, as in the survey area, where the depth of it has not been ascertained in the eastern part and thick blanket of Quaternary sediments are deposited, the error would appear easily in quantitative analysis of the basement in case of such a tendency that a large-scale geologic structure might be reflected.

Under these circumstances, the subsurface structure of the basement was analyzed in the survey assuming the geologic structure to be composed of two layers such as the basement rocks and the blanket formation overlying the former, which show a difference in density most distinctly. In this case, the average density of the basement was set to be  $2.6 \text{ g/cm}^3$  and that of the unconsolidated sediments including talus deposit, river sand and gravel of the Quaternary to be  $1.6 \text{ g/cm}^3$ , making the difference in density to be  $1.0 \text{ g/cm}^3$ . The basement structure in the case of  $0.8$  and  $1.2 \text{ g/cm}^3$  of density difference is also expressed in the analysis section, which would be instructive when the basement structure is made clear by drilling etc.

Fig. 2-41 shows the depth of basement. These show that the basement rocks are inclined toward the central part of the survey area with 10 to 20 degrees of inclination, and a 100-meter contour of the basement below the surface is parallel to the foot of the mountain where the basement rocks are exposed at a distance of one to 1.5 kilometers. The basement becomes generally depressed at the center of the survey area, and it is deeper on the southern side of the area



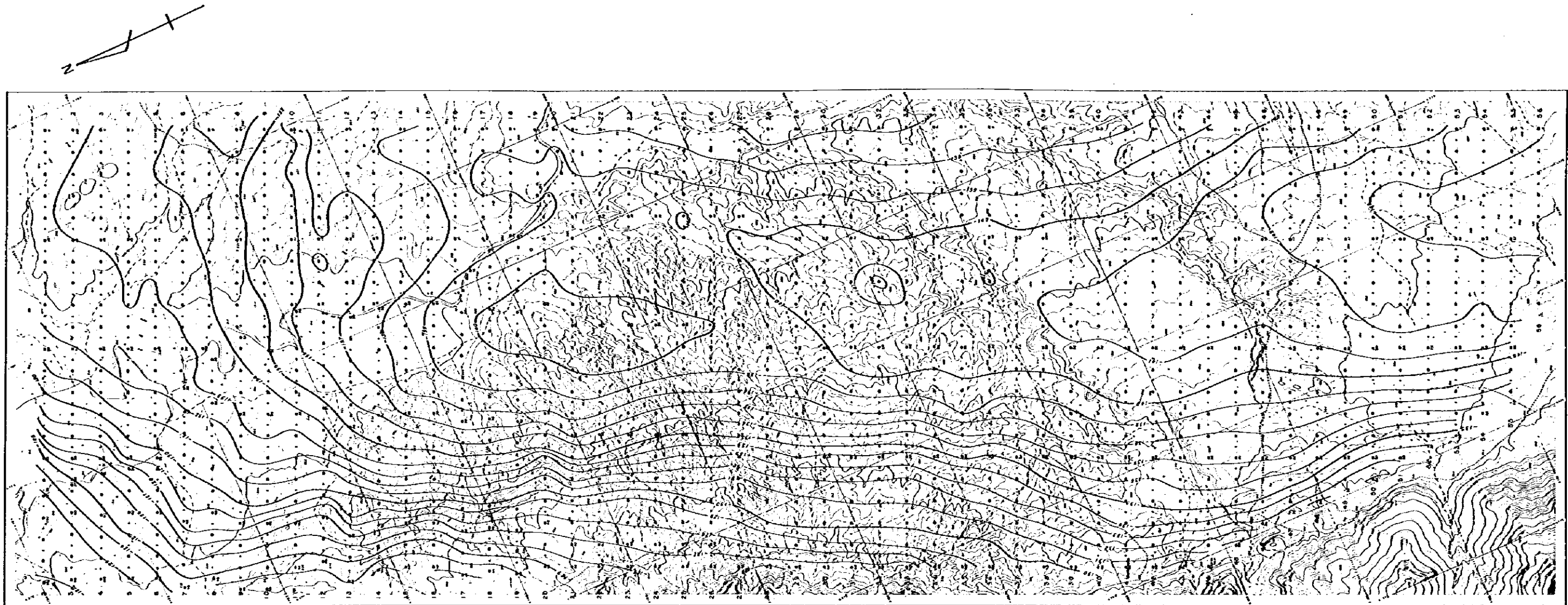


Fig. 2-37 Bouguer Anomaly Map ( $\rho=2.6\text{gt/cm}^3$ )

LEGEND

- Magnetic Observation Point and its Number
- ⊙ Magnetic and Gravity Observation Point and its Number
- 1 mgal
- - - 5 mgal





which is as deep as 200 meters below the surface on the southern side of the survey line 27. The deepest depression of the basement in the area deeper than 250 meters was analyzed at the central part of the survey lines 35 to 45 and on the eastern side of line 48 to 52. On the other hand, some swelling and projection or geologic structure having a higher density than the surrounding area was detected in the central part of the survey area where the basement becomes generally depressed. The swelling was indicated from No. 10 of the line 12 to No. 20 of the line 30, and the projections at No. 10 of the line 6, No. 26 of the line 40, No. 30 of the line 44 and No. 16 of the line 47. These anomalies are found at the places where they are detected as positive anomalies of residual gravity, leading to an assumption that these might indicate latent zones of intrusive rocks of high density.

### (3) Compilation

(a) The average density of the rock samples collected in the vicinity of the survey area was  $2.69 \text{ g/cm}^3$  in natural condition and  $2.71 \text{ g/cm}^3$  in wet condition except for chromite ore, and taking the cracks in the rock and correlation between the topography and the Bouguer anomaly into consideration, it seems reasonable to determine the average density of the rocks in the survey area to be  $2.60 \text{ g/cm}^3$ . In this connection the density of chromite ore was  $3.84 \text{ g/cm}^3$ , basaltic rocks  $2.80 \text{ g/cm}^3$ , serpentinites  $2.69 \text{ g/cm}^3$ , and the Mozambique metamorphic rocks constituting the basement  $2.57$  to  $3.07 \text{ g/cm}^3$ . On the other hand, although it is very difficult to assume the density of the Quaternary unconsolidated sediments, it was assumed to be about  $1.6 \text{ g/cm}^3$  because of plenty gravels contained in them. Therefore, from general point of view, it might be regarded that the density structure of the survey area is composed of the two layers of the basement rocks and the blanket sediments.

(b) The Bouguer anomalies of the survey area well reflect the geologic structure of the basement. On the western side of the area, a steeply inclined zone is formed reflecting the fault structure assumed to occur everywhere, indicating that the basement dips steeply toward the southeast. A low Bouguer anomaly is found in the central part of the survey area forming a narrow and long zone open to the south, suggesting that a boat-shaped basin structure of the basement was formed in this part. On the other hand in the northern part of the survey area the gravity contours swing to the east-west direction, which leads to an assumption that the geologic structure changes its trend to the direction of east to west in this part.

(c) Among the residual gravity anomalies with a wavelength of about one kilometer, positive anomalies considered to reflect the intrusive rocks of high density and fault structures of small to medium scale were detected, which suggests presence of the fault structure in the western part of the area and local swelling of the basement and latent mass of intrusive rocks in the

central part.

(d) It seems that the gravity basement of the survey area gradually increases its depth toward the center of the area to reach more than 250 meters below the surface. Some swellings of basement as high as several tens meters is considered to be present, which is almost consistent with the positive anomalies of residual gravity.

#### 2-5-4 Magnetic Survey

##### (1) Result of Survey

Maximum value of magnetic anomaly in the survey area was found to be 35,637 nT at point No. 29 of the survey line 9 and the minimum value 32,698 nT at No. 27 of the same survey line with a difference of 2,939 nT. The average magnetic value of the area seems to be about 34,000 nT. Fig. 2-38 shows the distribution of magnetic anomalies.

The magnetic anomalies of short period are distributed plentifully in the survey area, especially the anomalies with an amplitude of more than 500 nT were detected everywhere in the northern part of the area. However, the anomalies of short wave in the northern part are ranged in two rows being brought together. These groups of anomalies tend to be merged into one in the northeastern part of the survey area.

Since it is common that the strong magnetic anomaly is shown along the contact of the magnetic rock mass in such an area of low magnetic latitude ( $20^{\circ}\text{S}$ ) as in the survey area, these series of group of anomalies seems to indicate the contact of a large magnetic rock mass.

On the other hand, in the southern part of the survey area, the groups of magnetic anomaly with maximum amplitude of about 300 nT were detected, though not so strong as compared with those in the northern part. While the group of anomalies shows a north to south trend in the northern side, it is ranged northeastward on the southern side. It is also assumed that these groups of anomalies have caught a part of the contact of a magnetic rock mass.

##### (2) Results of Analysis

The results of analysis are shown on Fig. 2-40 and Fig. 2-41.

The magnetic anomalies expressed on the magnetic maps form a complicated anomalous zone consisting of high anomalies and low anomalies on a small scale. The anomalous zone detected in the northeastern part of the survey area is particularly complicated, and it is likely that the rock masses are inclined, that the susceptibility is greatly varied locally, that natural remnant magnetism (NRM) would be present and that the position of the mass is deeper or shallower than that the anomalies represent a larger homogeneous magnetic rock mass. The

calculation on analysis of magnetism is limited in case of such a complicated magnetic distribution, and the analysis is made in such a case with an assumption that these represent a large homogeneous magnetic mass.

Thus it might be a better interpretation to regard the analyzed magnetic mass to include the intrusive rocks with magnetism in a rough-and-ready way.

On the other hand, if there is no NRM detected in the magnetic rock mass in the area having a magnetic inclination of  $20^{\circ}\text{S}$  as in the survey area, positive anomaly will be shown at the contact on the northern side and negative anomaly on the southern side (Fig. 2-38). The ratio of the magnitude of the positive anomaly and negative anomaly varies with the shape of inclination of the magnetic rock mass.

Two series of magnetic rock masses were analyzed in the northern part of the survey area and one series in the southern part. The mass on the eastern side in the northern part is 100 to 500 meters wide and about six kilometers long with the trend of  $\text{N}50^{\circ}\text{E}$  to  $\text{N}20^{\circ}\text{E}$ , and that on the western side is 200 to 400 meters wide extending in the direction of  $\text{N}60^{\circ}\text{E}$  for about two kilometers. Among the magnetic masses, the one on the eastern side dips northwestward in a low angle (about ten degrees) and the other on the western side dips  $20^{\circ}$  to  $30^{\circ}$  toward the southeast, the opposite side of the above. According to the aeromagnetic survey conducted in advance of this survey, these two series of magnetic anomaly zones were caught as two large magnetic anomalies showing different forms.

The magnetic rock mass detected from the aeromagnetic anomalies is analyzed at the center put between the two series of magnetic anomalies as shown in Fig. 2-39. It seems that the magnetic rock mass analyzed from the aeromagnetic anomalies represents the part of intrusive vent corresponding to the root of the magnetic rock at relatively deeper part and that the two series of magnetic anomalies analyzed from the ground magnetic prospecting would represent the thinly extended part of the periphery of the mass taking funnel-like form at a shallow part. The depth of the magnetic rock masses analyzed from the ground magnetic prospecting is 50 to 200 meters below the surface and that of the one analyzed from the aeromagnetic survey is deeper than 250 meters below the surface.

While the magnetic rock mass detected in the southern part of the survey area was analyzed as the mass 100 to 400 meters wide and more than four kilometers long extending  $\text{N}40^{\circ}\text{E}$  to  $\text{N}10^{\circ}\text{W}$  on the whole, it is considered that it could be divided into three parts and that these parts are bordered by fault-like structures which are discontinuous magnetically. All these masses dip westward, and those on the northern side and the southern side show a low angle of  $10^{\circ}$  to  $20^{\circ}$  and the one at the center takes a high angle of  $60^{\circ}$  to  $90^{\circ}$ . Aeromagnetic anomaly was also de-

tected at the position corresponding to the magnetic anomalies in the southern part, and the magnetic rock mass analyzed from the aeromagnetic anomalies seems to correspond to the core which will be the root of intrusive rock, showing a depth deeper than 300 meters, and the one analyzed from the ground magnetic prospecting seems to correspond to the expanded part of an umbrella of the mass in the shallow part.

### (3) Compilation

(a) The average values of magnetic susceptibility of the rock samples distributed in the vicinity of the survey area and collected in the survey are as follows (Table 2--27):

121.3 ~ 321.1 x 10<sup>-6</sup> cgs. emu in the basement rocks (Mozambique metamorphic rocks).

For intrusive rocks, 202.05 x 10<sup>-6</sup> cgs. emu in granite and 197.1 x 10<sup>-6</sup> cgs. emu in gabbro.

These are small in value.

4,532.6 x 10<sup>-6</sup> cgs. emu in serpentinite, showing by far the great value.

435.5 x 10<sup>-6</sup> cgs. emu in basalt lava. Although this is relatively large in value, it is small compared with common basalt (an order of 10<sup>-3</sup>).

Strong magnetic anomaly detected in the survey area seems to be caused by serpentinites, and a part of strong susceptibility in basalt may have formed the anomaly.

(b) Altogether three magnetic anomalies including the two series of them in the northern part and a series in the southern part, were detected in the survey area. The anomaly on the eastern side in the northern part extends for six kilometers in the NNE to SSW trend and the one on the western side in the same part for two kilometers in the NE to SW trend have been strongly detected.

On the other hand, the anomaly group in the southern part shows a small amplitude, leading to an assumption that the magnetic rock mass analyzed from the above would be emplaced in the relatively deeper part or would have low susceptibility.

(c) The magnetic rock mass analyzed from the groups of magnetic anomalies can be classified as dykes several hundred meters wide and several kilometers long.

Those in the northern part are assumed to dip at low angle facing each other and to be joined together in the deeper subsurface. On the other hand, those in the southern part are assumed to dip westward and to be latent to the southwest of the survey area.

(d) The results of the aeromagnetic survey and that of the ground magnetic prospecting at this time are in consistent with each other in a general way. However, the forms of magnetic rock masses analyzed from those anomalies are different from each other. In contrast to that the anomalies of the ground magnetic prospecting are strongly shown at the contact of the magnetic rocks in the zone of low latitude of the earth's magnetism in the survey area, it is considered that the aero-



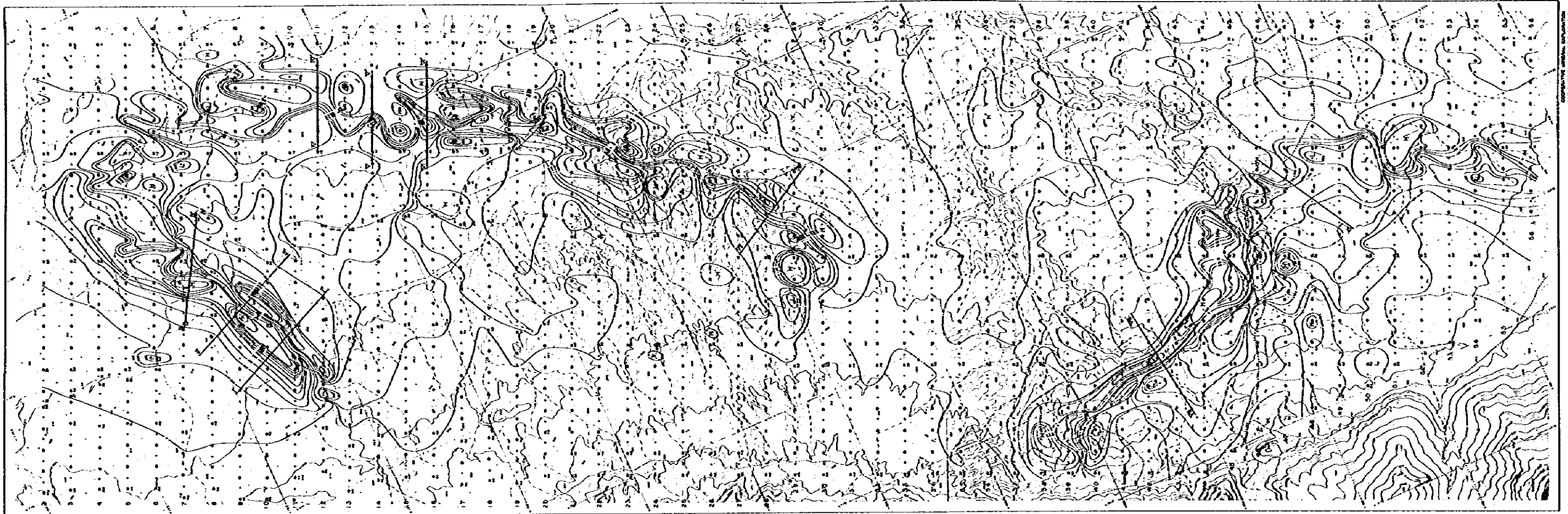
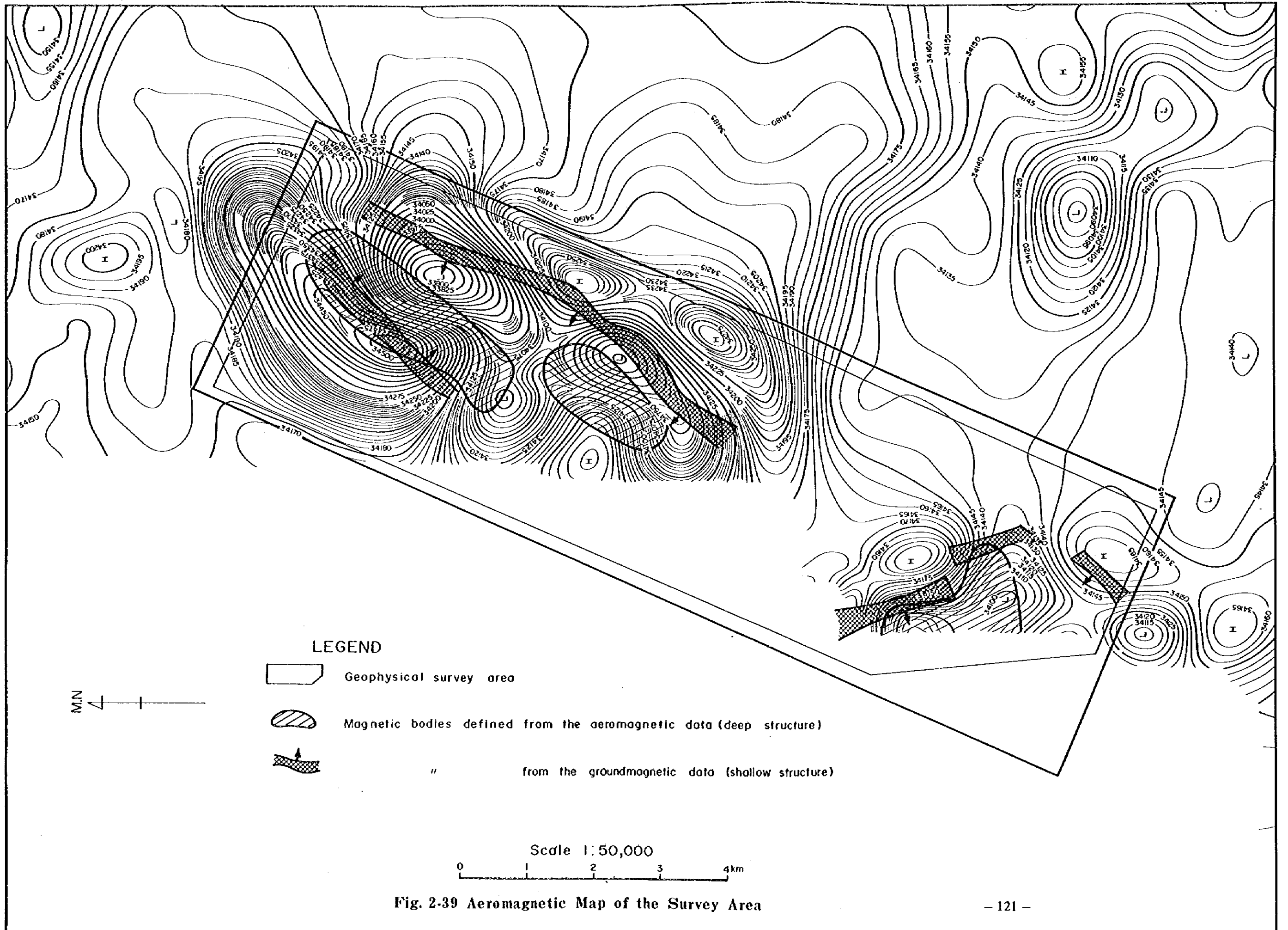


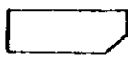


Fig. 2-38 Total Magnetic Intensity Map

LEGEND

- Magnetic Observations Point and its Value
- Magnetic and Gravity Observations Point and its Value
- 100 : (150000 ± 100) G
- ~ : 100 G
- ~ : 50 G
- H : High Anomaly
- L : Low Anomaly



**LEGEND**

-  Geophysical survey area
-  Magnetic bodies defined from the aeromagnetic data (deep structure)
-  " from the groundmagnetic data (shallow structure)

M.N.  
↑

Scale 1:50,000  
0 1 2 3 4km

**Fig. 2-39 Aeromagnetic Map of the Survey Area**





magnetic anomaly obtained from high altitude of measurement would strongly reflect the central part of the rock mass. And this is the reason why they differ from each other. From these fact, it is highly possible that the magnetic rock mass analyzed from aeromagnetic anomaly would show the central part of the intrusive rock with high susceptibility and the position of the magnetic rock analyzed from ground prospecting would indicate the peripheral part of the intrusive rock.

#### 2-5-5 Summary of Geophysical Survey

(1) The surveyed area lies within the Rift Valley separated from the block on the west by fault escarpment, and the geologic structure of NE-SW system seems to be notable based on the rows and trend of the intrusive rocks and the distribution of gravity.

(2) The distribution of gravity in the survey area markedly reflects the geologic structure of the basement, and a steep inclination of gravity is formed on the western side of the area reflecting the fault structure dipping southeastward.

On the other hand, the central part of the survey area forms a low gravity zone, which leads to an assumption that the basement has been depressed in the central part of the survey area. The bottom of the depression reaches 250 meters below the surface when the difference in density between the basement rocks and the blanket sediments overlying the former is assumed to be  $1.0 \text{ g/cm}^3$ .

(3) From the residual gravity anomaly, fault-like structure and presence of latent intrusive rocks, and swell of basement are assumed in the basement structure.

(4) According to the test on physical properties of the rock samples collected in the survey area, the density of chromite ore is the highest showing the average value of  $3.84 \text{ g/cm}^3$  and those of the Mozambique metamorphic rocks of the basement are shown to be 2.57 to  $3.07 \text{ g/cm}^3$ . In terms of the intrusive rocks, gabbro shows  $2.94 \text{ g/cm}^3$  followed by  $2.69 \text{ g/cm}^3$  for serpentinite, and granite shows the lowest value of  $2.52 \text{ g/cm}^3$ . Basalt shows  $2.80 \text{ g/cm}^3$ .

As to magnetism of the rocks, serpentinite is as strong as  $4,532.6 \times 10^{-6}$  cgs. emu followed by basalt showing a value of  $435.5 \times 10^{-6}$  cgs. emu, which is lower than ordinary basalt. The basement rocks and other intrusive rocks show weak magnetism of 121.3 to  $382 \times 10^{-6}$  cgs. emu.

(5) Three large groups of magnetic anomalies are detected in the survey area, two series in the northern part and one in the southern part. Two intrusive rock masses are assumed to be present in the northern part and one mass in the southern part corresponding to the above respectively.

(6) It is inferred that the center of a latent intrusive rock of high susceptibility is located at depth lower than 250 meters below the surface. It is highly possible that the intrusive rock of high susceptibility would be ultrabasic rocks including serpentinite. In this case, potentiality of chromite ore deposit is expected.

Judging from the scale of latent rock mass, and the ore reserves of the known ore deposits occurring in the Telot serpentinite mass in the vicinity of the survey area, it appears the potential ore deposit is composed of small podiform chromite bodies and the exploration work to get sufficient ore reserves is difficult because of small scale of ore bodies and the deep seated nature of the basal rocks. Moreover, the rock mass is found underneath the soft alluvial formation, and the Wei-Wei River with plenty water flows at the central part of the mass. Therefore it would be difficult to design for open pit mining from the topographical restriction and the depth. Further, when taking the infrastructure into account, mine development might not be economically viable.

However, in case the exploration for the rock mass of high magnetism to be continued by drilling and other methods in future, it is recommendable that the exploration work be conducted for the rock mass of high magnetism in the northern part of the survey area, to select the target, where the depth of potential occurrence of intrusive rock is expected to be shallow.



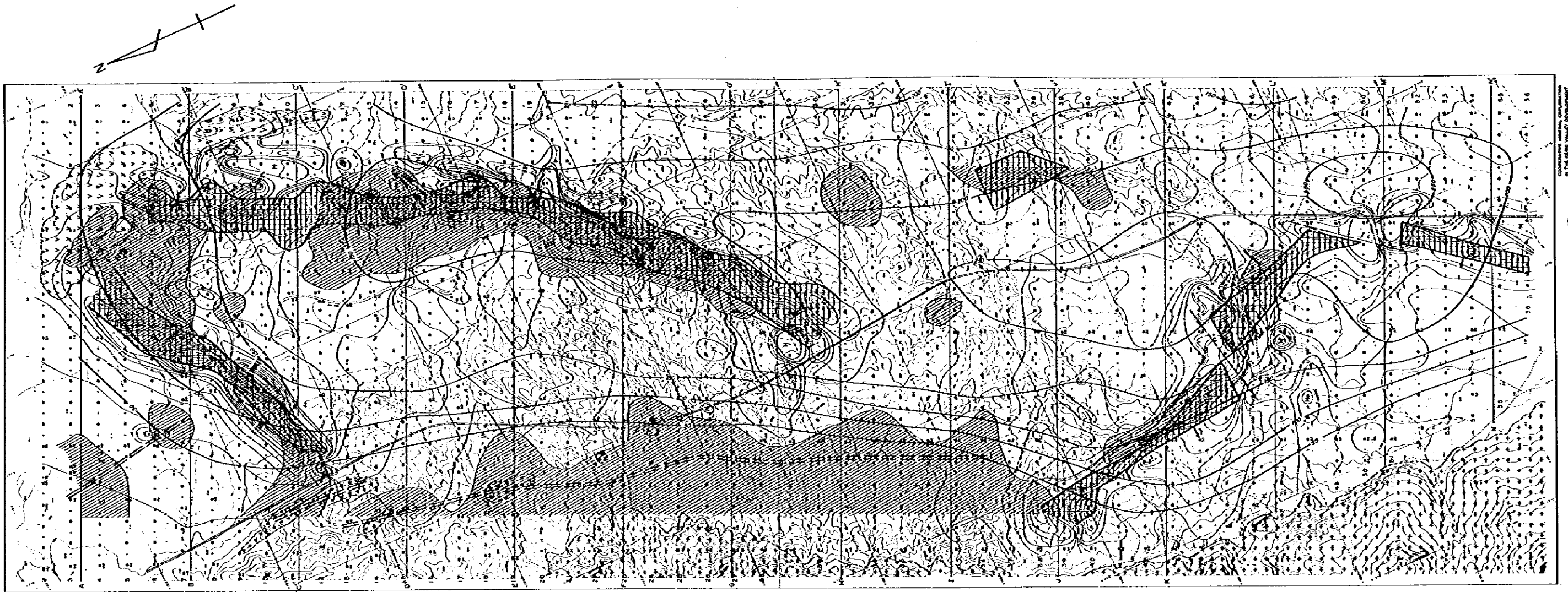
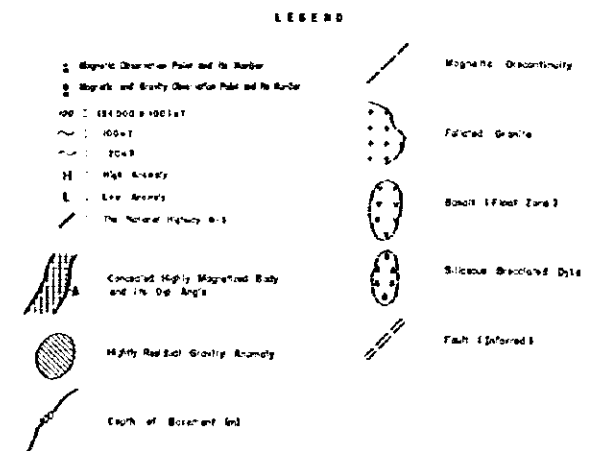


Fig. 2-40 Interpretation Map (Plane)



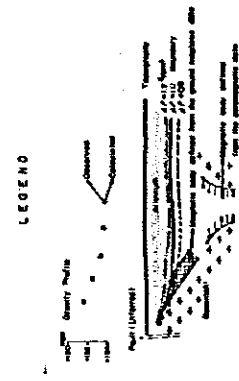
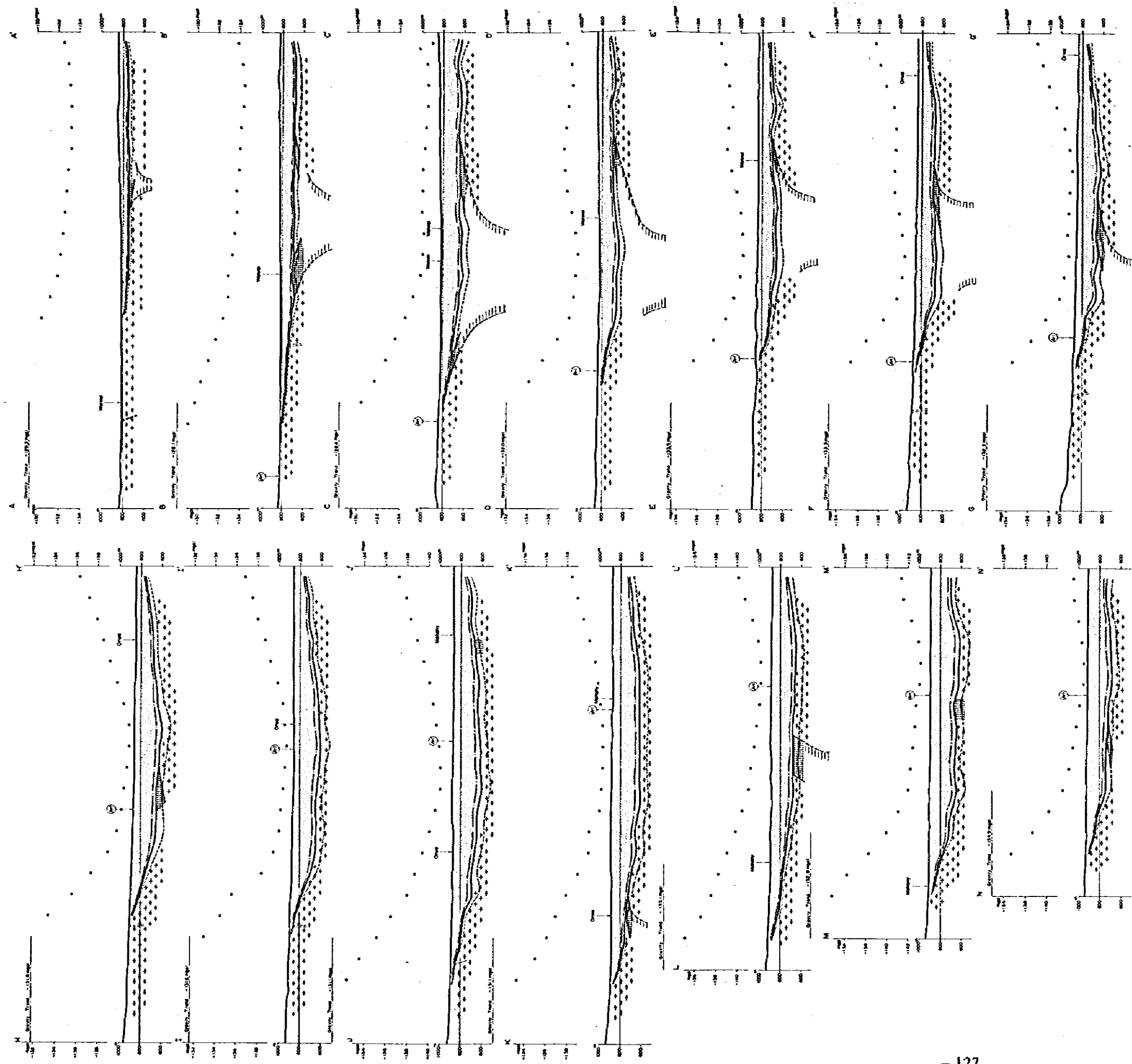


Fig. 2-41 Interpretation Map (Section)



## CHAPTER 3 CONCLUSION AND RECOMMENDATION

### 3-1 Conclusion

The following conclusions are obtained based on the results of the three years survey.

#### (1) Regional Survey Area

There are several alluvial and eluvial gold deposits in the area, which were also detected by the geochemical survey of the project. They are, however, not large-scale deposits suitable for systematic mining operation. The present small-scale style of digging and panning gold by the local people is hence justified for those deposits.

Known copper showings and copper and molybdenum showings newly found by the survey are all small in scale, and have little value for further exploration work at the present status of economy.

Mineralization of metal except gold is judged to be relatively weak throughout the area from both results of geological and geochemical survey, and thus exploration target on metal should be limited mainly to gold.

#### (2) Semi-detailed Survey Area A, Detailed Survey Area

The chromite, garnierite and eluvial gold deposits are emplaced in the Telot serpentinite body.

The ore reserves of the chromite deposit is calculated to be 8,400 tons ( $\text{Cr}_2\text{O}_3$ : 48%) of both proved and probable ore reserves altogether by the past exploration work including diamond drilling. The deposit has high chromium grade and suitable for open pit mining, but scanty in ore reserves, so that the deposit would not be economically feasible for exploitation at the present status of economy. The possibility of locating more ore bodies at the surface and shallow zones which are suitable for open pit mining is little judging from the results of the geological and geochemical survey by this project.

Garnierite nickel deposits form sizable mineralized zones at four places in weathered parts of the serpentinite body. The calculation of ore reserves conducted by the Department of Mines and Geology of Kenya (presently Mines and Geological Department) gives about five million tons (a little more than one percent in nickel content) of probable ore reserves and about fourteen million tons (0.7 percent in nickel grade) of possible ore reserves, which is considered to be reasonable on the basis of the result of survey of this project. But the terrain of the mineralized zones is ragged and steep, and it is pointed that the mineralization is pretty irregular and the high grade zones are sporadic. The deposit is low in nickel grade and scanty in ore reserves compared

with other deposits of this kind elsewhere in the world. Moreover, the deposits are situated far away from the coast for shipment and infrastructure conditions would need to be improved. Therefore, it does not appear to be worthy of further exploration work.

The eluvial gold deposits occur in the silicified zone extending two kilometers northwards with a width of 350 meters in the central zone of Telot serpentinite body, which is almost consistent with the geochemical anomalous zone of gold. The gold content in the high grade parts of the deposit is estimated to be approximately 1 g/ton and less than 0.5 g/ton as a whole, and the estimation leads to the conclusion that the deposit could not be operated by systematic mining methods. However, it is expected that the area to the south of the present mining site, currently being mined by hand by the local residents, where silicified zone and the geochemical anomalous zone are overlapping, would be the next mining site for them.

No large-scale mineralization besides the Telot deposits has yet been discovered in the area.

### (3) Semi-detailed Survey Area B

No further exploration is recommended for the area because the survey indicated that pegmatites occurring in the area are barren of any useful metals.

### (4) Area C

The northern rock mass among those detected by airborne magnetic survey conducted by MGD has high possibility to be serpentinites judging from the results of the ground magnetic and the gravity survey.

The potential chromite deposits which may occur in the serpentinite body are inferred to comprise small podiform bodies judging from the estimated scale of the rock mass and the occurrence of the chromite deposits in the Telot body. The exploration work to get sufficient ore reserves for mining operation is, then, thought to be pretty difficult because of small size of ore bodies, and deep position of the rock mass under the superficial overburden.

## 3-2 Recommendation

Although the cooperative mineral exploration survey in the Kerio Valley Development Authority Area by the Japanese government will be completed by the end of 1985, the following surveys by Kenyan side are proposed as recommendation for the ore deposits and showings which have been clarified by this survey.

(1) Various kind of economic minerals such as gold, chromite, nickel, copper and molybdenum occur in the area, but they are all small in scale or low in grade. Thus compact and small scale exploitation is recommended for those deposits or showings.



**(2) Chromite Deposit at Telot**

The deposit is scanty of ore reserves but high in chromium grade and suitable for open pit mining, so that operation on a small scale would be recommended when market conditions improve and demand on chromite arises in Kenya.

**(3) Gold Deposit at Telot**

Geochemical tests of rock samples is recommended to know the possibility of targeting next mining sites to the south of present digging places where the silicified zone and anomalous zone overlap.

**(4) Area C**

Exploration work to locate chromite ore bodies is estimated to be quite difficult, but in case that further exploration, for example, drilling work etc., is introduced, the target area should be limited to the north part where the depth of concealed rock mass is expected to be shallow.

The ground geophysical survey comprising magnetic and gravity methods in the area C revealed the characteristic of the latent magnetic bodies which were detected by the airborne geophysical survey conducted by Mines and Geological Department.

The result is a good example in which ground geophysical survey following airborne survey led to the evidence of the occurrence of serpentinite bodies which might have chromite deposits, though further exploration work are considered to be difficult because of topographic restriction in this case.

The model established by this type of ground geophysical survey could be used to define the existence of serpentinite bodies in areas where anomalies similar to the one investigated have been delineated by airborne geophysical survey.

